ARTICLE

Check for updates

Nutrient use efficiency has decreased in southwest China since 2009 with increasing risk of nutrient excess

Guitang Liao [1,2✉], Yongdong Wang[2], Haiying Yu[2], Peng He[3], Zhengyu Lin[3], Tianfei Dai[4], Chenghua Xu[1] & Tinxuan Li[2✉]

The optimal application of nutrients, such as nitrogen and phosphorus, to the soil is crucial for achieving high crop yields with minimal environmental impact. However, the effect of spatio-temporal changes in soil nutrient supply on crop yield is poorly understood in China. Here, we present a framework that combines environmental data, fertilizer field experiments, and machine learning to estimate the rice yield responses to different nutrient conditions and overall farmland nutrient sustainability in southwest China from 2009 to 2019. The results show that the fertilizer input has contributed to the long-term increase in rice yield over the past ten years. The fertilizer use has increased rice yield by 2.3–2.4 tons per hectare per year. However, the nutrient use efficiency decreased, with the fertilizer contribution ratio declining from 29.3% in 2009 to 27.5% in 2019. Further, 19% of the rice-growing farmlands are at risk of nutrient excess, and 36% are at risk of nutrient degradation. Controlling nitrogen and phosphorus input is key to nutrient regulation, and our approach may guide the sustainable use of nutrient resources on farmlands.

[1] College of Resources and Environment, Chengdu University of Information Technology, Chengdu 610225, China. [2] College of Resource, Sichuan Agricultural University, Chengdu 611130, China. [3] Agricultural Information and Rural Economy Research Institute, Sichuan Academy of Agricultural Sciences, Chengdu 610066, China. [4] Sichuan Green Food Development Center, Chengdu 610041, China. ✉email: lgt@cuit.edu.cn; litinx@263.net

Food is the material basis for the sustainable development of human society. Since the coronavirus disease (COVID-19) pandemic, food security issues have gained wider attention and have been more extensively discussed around the world[1,2]. Fertilizers, especially the widespread use of chemical fertilizers, have been one of the key factors in food production over the past 50 years and have enabled global food quantities to meet the needs of population growth[3–5]. However, the resource and environmental costs required to achieve the above goals are extremely high[6,7], with rice, wheat, and maize alone producing around 60% excess nitrogen and phosphorus[8]. A sobering prediction indicates that the demand for global food production will double by 2050, putting unprecedented pressure on the global ecosystem[9]. How to ensure ecological security while achieving food security, has become an important challenge for global sustainable development[10–13].

For decades, China has fed 22% of the world's population with only 9% of the world's arable land, making a huge contribution to global food security but resulting in higher environmental costs and resource consumption[14]. It is estimated that the contribution rate of chemical fertilizers to crop yield once reached 50% in China[15,16]. However, due to long-term excessive and unbalanced fertilization, the amount of fertilizer per unit area in China was three times that of the EU and the US, resulting in soil degradation, non-point source pollution, low fertilizer utilization, and other serious problems[17,18]. Taking effective measures to reduce the number of chemical fertilizers and adjust the nutrient structure has become an important part of China's sustainable development strategy in recent years[19,20]. Although China has achieved zero growth in the total amount of chemical fertilization at the national level, there is great spatial heterogeneity and seasonal variation in soil nutrient conditions and fertilizer management in different regions, which makes fertilizer pollution control complicated and difficult at the regional scale[21,22]. Therefore, an accurate assessment of nutrient use efficiency and its impact on crop yield at the regional scale is of great significance for food security and sustainable development in China and the world[23–25].

Currently, scholars have developed various mathematical models to predict the effects of environmental factors on crop yield: (1) Meteorological yield model. This model uses factors such as light, temperature, and water to build a statistical or mechanism model and then combines climate prediction to simulate crop yield; its prediction accuracy depends largely on the accuracy of meteorological data[26–29]. In addition, agro-hydrological models such as CERES[30], SWAP[31], and AquaCrop[32] have also been widely used to assess the impact of climate change on crop yield[33,34]. (2) Remote sensing yield model. This model is based on the differences in the spectral characteristics of crops at different growth stages and uses remote sensing data bands to establish a model of their quantitative relationship with crop biomass to achieve rapid and accurate large-scale crop yield estimation[35]. As early as the 1980s, the United States and Europe began using Landsat data to estimate crop yield on global and national scales[36,37]. In recent years, researchers have widely used optical remote sensing data (TM, ETM+, NDVI, EVI, etc.)[38,39], hyperspectral remote sensing data (MODIS)[40], microwave remote sensing data (FPAR)[41], and agronomic parameter data (LAI, NPP, etc.)[42] to estimate the yield of crops such as rice and winter wheat, and the prediction error is usually 10–20%. (3) Crop growth model. This model can quantitatively evaluate the interactions of crop yield and its influencing factors by simulating crop growth processes such as light energy utilization, phenological development, dry matter distribution, and nutrient balance, and the prediction error is usually around 10%[43]. Currently, widely used crop growth models include DSSAT[44], WOFOST[45], APSIM[46], ORYZA[47], CropGrow[48], etc. Notably, the application of crop growth models at the macro scale is limited due to the large number of model parameters, some of which are difficult to obtain. (4)

Machine learning (ML) models. With the advancement of artificial intelligence technology, crop yield prediction models that integrate multi-source environmental data and ML algorithms have been the frontier and hotspot of precision agriculture research[49]. Scholars have selected various factors (climate (temperature, humidity, precipitation, solar radiation, etc.), soil (type, moisture, texture, etc.), topography (elevation, slope, etc.), crops (variety, density, etc.), and management (cultivation, irrigation, etc.)[50–54]) using ML algorithms (e.g., neural networks[55], random forests[56], support vector machine[57], extreme gradient boosting[58], and long-short term memory[59], etc.) to effectively improve the accuracy of crop yield prediction. In addition, some scholars have studied the impact of soil nutrients on crop yield at global and national scales to estimate fertilizer requirements and formulate fertilization strategies, usually with low spatial resolution (≥500 m)[60–62]. Unfortunately, most of the current prediction models cannot explain the impact of changes in soil nutrient supply on crop yield[63]; in particular, the temporal–spatial accurate simulation of crop yield based on fertilizer response on the regional scale is rarely reported.

Since 2005, a large number of fertilizer response field experiments have been conducted in China[24], but the application of the results has been limited to fitting the fertilizer response function model[64] to calculate the optimal fertilization rate of crops, and the value of the experimental data in crop yield prediction has not been deeply explored[65]. On the other hand, the Chinese government started to implement fertilizer reduction actions in 2015, and then some scholars attempted to evaluate the fertilizer reduction potential at the national[66], provincial[67–69], and county[70] scales. However, these studies generally lack effective methods to link microscopic field experiments and macroscopic spatial simulations, which still rely on the results of single-point experiments or the average value of multi-point experiments, leading to gaps in the precise management of farmland nutrients at the regional scale[71]. Therefore, we developed a new model to estimate crop yield responses under different nutrient conditions by integrating fertilizer response field experiments, multi-source environmental data, and ML algorithms, using the main rice-growing area in southwest China as an example, to (1) upscale and spatialize multi-point fertilizer field experiments, (2) accurately simulate the contribution of fertilizer to rice yield, and (3) spatially identify and assess farmland nutrient sustainability.

Results

Rice yield GWRK model. Based on the fitting modeling of 1027 field experiment training samples using ArcGIS, the Geographically weighted regression (GWR) models of soil-based yield and relative yield coefficient (RYC) were established (Supplementary Tables 1–3). The R^2 of the GWR models of soil-based yield and RYC were 0.41 and 0.49, respectively. After ordinary kriging correction of the GWR model residuals (Supplementary Table 4), the spatial distributions of the regression coefficients of the geographically weighted regression kriging (GWRK) model variables are shown in Supplementary Figs. 1 and 2. The regression coefficient of each model variable contained positive and negative values, indicating that the influence of each environmental variable on the spatial distribution of rice yield showed spatial heterogeneity. Sensitivity analyses showed the stability of the soil-based yield (YS) and the RYC model parameters (Supplementary Table 5 and Supplementary Fig. 3). The relative sensitivity index (RSI) of the model metrics was less than 0.3, except for TEM and PRE, which had high sensitivity (RSI > 0.85.) Therefore, when the rice yield model is applied to different climatic regions, the meteorological metrics should be calibrated. According to the evaluation indexes in Table 1, the prediction accuracies of the YS and fertilized yield (YF) GWRK models were close, and the prediction accuracies of YF were better than those

Table 1 Evaluation indexes of prediction accuracy of GWRK models.

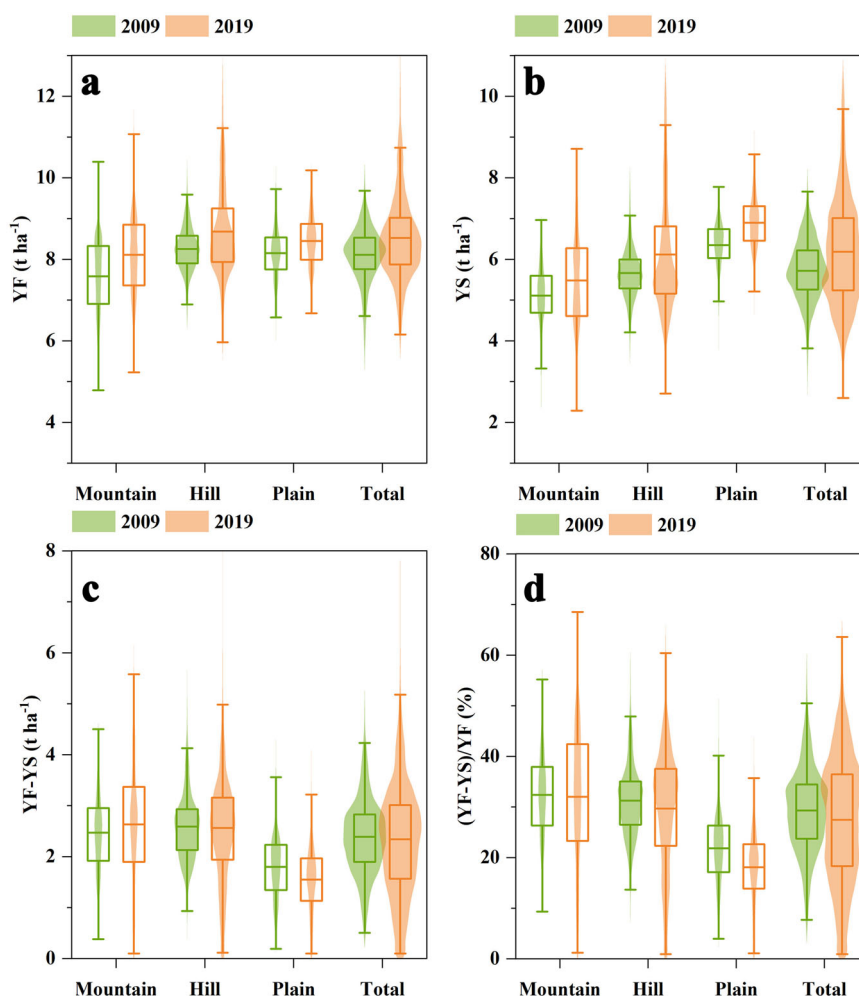| Model	Region	Number of samples	ME (t ha-1)	MAE (t ha-1)	RMSE (t ha-1)	SMAPE (%)
YS GWRK	Total	155	−0.21	0.89	1.22	16.49
	Plain	38	−0.57	0.97	1.23	16.37
	Hill	97	−0.04	0.86	1.11	15.54
	Mountain	20	−0.37	0.92	1.62	21.29
YF GWRK	Total	155	−0.20	0.89	1.22	11.45
	Plain	38	−0.37	0.80	1.00	9.76
	Hill	97	−0.15	0.83	1.06	10.51
	Mountain	20	−0.17	1.29	2.01	19.01

Fig. 1 Statistical chart of rice yield from 2009 to 2019 in different regions of Sichuan Basin, SW China. Fiddle plots of (**a**) rice soil-based yield (YS), (**b**) fertilized yield (YF), (**c**) fertilizer increased yield (FIY), and (**d**) fertilizer contribution ratio (FCR) for all grids (4.87 × 10⁶). Boxes represent interquartile range with the mean value as the bold line, whiskers represent 1.5 interquartile range, and the outer border represents the data distribution.

of YS, reflecting that fertilizer input effectively improved the stability of crop yield in the study area[63]. The ME values of both models were negative, indicating that the predicted yields of the models were slightly higher than the observed yields. The SMAPE of soil-based yield in hills and plains ranged from 15% to 17%, while the SMAPE of fertilized yield was only about 10%. However, the SMAPE of yield forecast in mountainous areas was between 19% and 22%.

Rice yield distribution characteristics. From 2009 to 2019, the rice yield showed an increasing trend in the study area (Fig. 1, Supplementary Table 6). The average YS increased from 5.72 t ha⁻¹ in 2009 to 6.19 t ha⁻¹ in 2019, which was highest in plains, followed by hills and mountains. From 2009 to 2019, YS in the study area increased by an average of 0.47 t ha⁻¹, with plains, hills, and mountains increasing by 0.55 t ha⁻¹, 0.46 t ha⁻¹, and 0.38 t ha⁻¹, respectively. The average YF increased from 8.11 t ha⁻¹ in 2009 to 8.53 t ha⁻¹ in 2019, which was highest in hills, followed by plains and mountains. YF increased by an average of 0.42 t ha⁻¹, with plains, hills, and mountains increasing by 0.3 t ha⁻¹, 0.43 t ha⁻¹, 0.53 t ha⁻¹, respectively. The average fertilizer increased yield (FIY) was about 2.3–2.4 t ha⁻¹, which was significantly lower in plains than in hills and mountains. From 2009 to 2019, the average FIY decreased by 0.05 t ha⁻¹, with decreases by 0.25 t ha⁻¹ and
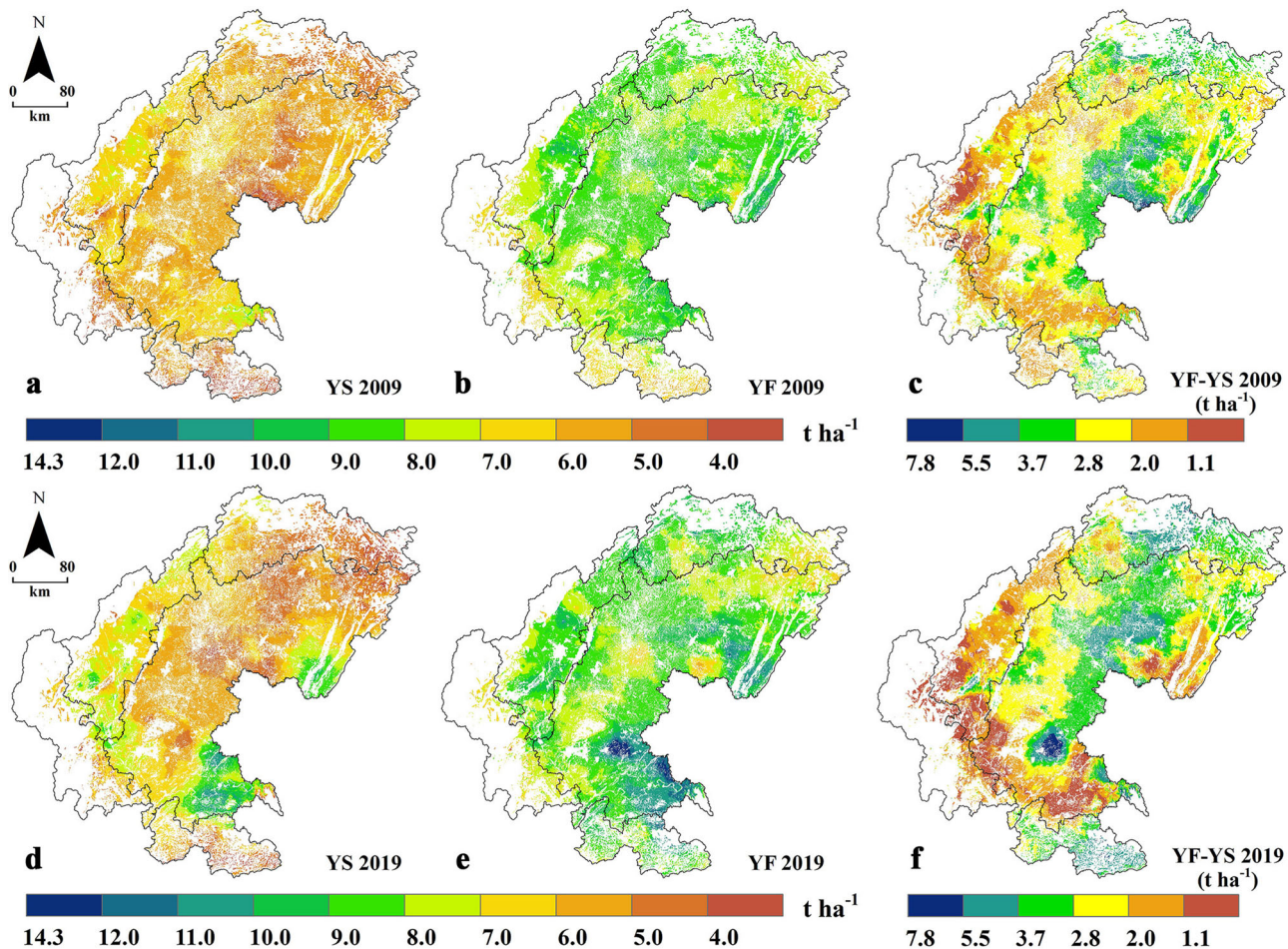
Fig. 2 Spatial distributions of rice yield from 2009 to 2019 in the Sichuan Basin, SW China. Spatial distribution of (**a**) YS, (**b**) YF, (**c**) FIY in 2009 and (**d**) YS, (**e**) YF, (**f**) FIY in 2019.

0.03 t ha⁻¹ in the plains and hills, respectively, and an increase by 0.16 t ha⁻¹ in the mountains. In particular, fertilizer inputs brought YF in the hills to the level of the plains. The average fertilizer contribution ratio (FCR) was 27–29% in the study area, with mountains > hills > plains, which is in consistent with the findings of Liang, et al.[72]. Moreover, the standard deviation of YF was lower than that of YS. This indicates that fertilizer inputs have positively contributed to the growth and stability of rice yield in the study area over the past 10 years. However, we could also see that the effect of fertilization on rice yield in the study area had a downward trend. The average FIY decreased from 2.39 t ha⁻¹ in 2009 to 2.34 t ha⁻¹ in 2019. FCR decreased from 29.3% in 2009 to 27.5% in 2019. Except for mountainous regions, the growth rate of YF was lower than that of YS. Particularly in the plains, the FIY and FCR decreased by nearly 14% and 17% respectively.

Figure 2 shows that the spatial distribution of the rice yield levels in 2009 and 2019 was similar, and the overall trend was plains > southern hills > eastern hills > central hills > northern mountains > southern and southwestern mountains. The regions with high YS were mainly distributed in the western plains and southern hill. The regions with high YF are concentrated in the central plains, south and eastern hills. The spatial distribution of FIY is regular from 2009 to 2019. The low FIY area was distributed in a band along the plain-Minjiang River-Yangtze River, and the area with high FIY was mainly concentrated in the central and northeastern part of the hills, the northern and southern part of the mountains. Meanwhile, the change in FIY showed significant spatial heterogeneity. The northern and

southern plains, and the eastern, southern, and southwestern hills mainly showed negative changes, and the central and northern hills and mountains mainly showed positive changes. The order of FIY changes from high to low was central hills > northern hills > mountains > plains > southern and southwestern hills. In the Sichuan Basin, FIY decreased in more than 50% of the regions, and the proportions of areas with decreased FIY were 68.3%, 46.8% and 43.2% in the plains, hills and mountains, respectively.

Rice nutrient balance distribution characteristics. In this paper, the average of Sichuan Basin was used and the nitrogen, phosphorus and potassium uptake were 2.03 kg, 0.92 kg and 2.47 kg, respectively (Supplementary Figs. 4, and 5, Supplementary Tables 7 and 8). The average nitrogen fertilizer utilization efficiency (REN), phosphorus fertilizer utilization efficiency (REP), and potassium fertilizer utilization efficiency (REK) in the Sichuan Basin were 28.94%, 13.17%, and 26.38%, respectively (Supplementary Fig. 6 and Supplementary Table 9). The distribution of fertilizer utilization efficiency was similar, with hills > mountains > plains in general. The areas with high fertilizer utilization efficiency were mainly distributed in the north-eastern hills and northern mountains. However, the fertilizer utilization efficiency is generally low in the region along the plains-Minjiang River-Yangtze River. The average theoretical nitrogen fertilizer rate (TFRN), theoretical phosphate fertilizer rate (TFRP), and theoretical potassium fertilizer rate (TFRK) were 125.8 kg ha⁻¹, 63.4 kg ha⁻¹, and 90.1 kg ha⁻¹ in 2009, respectively; the average
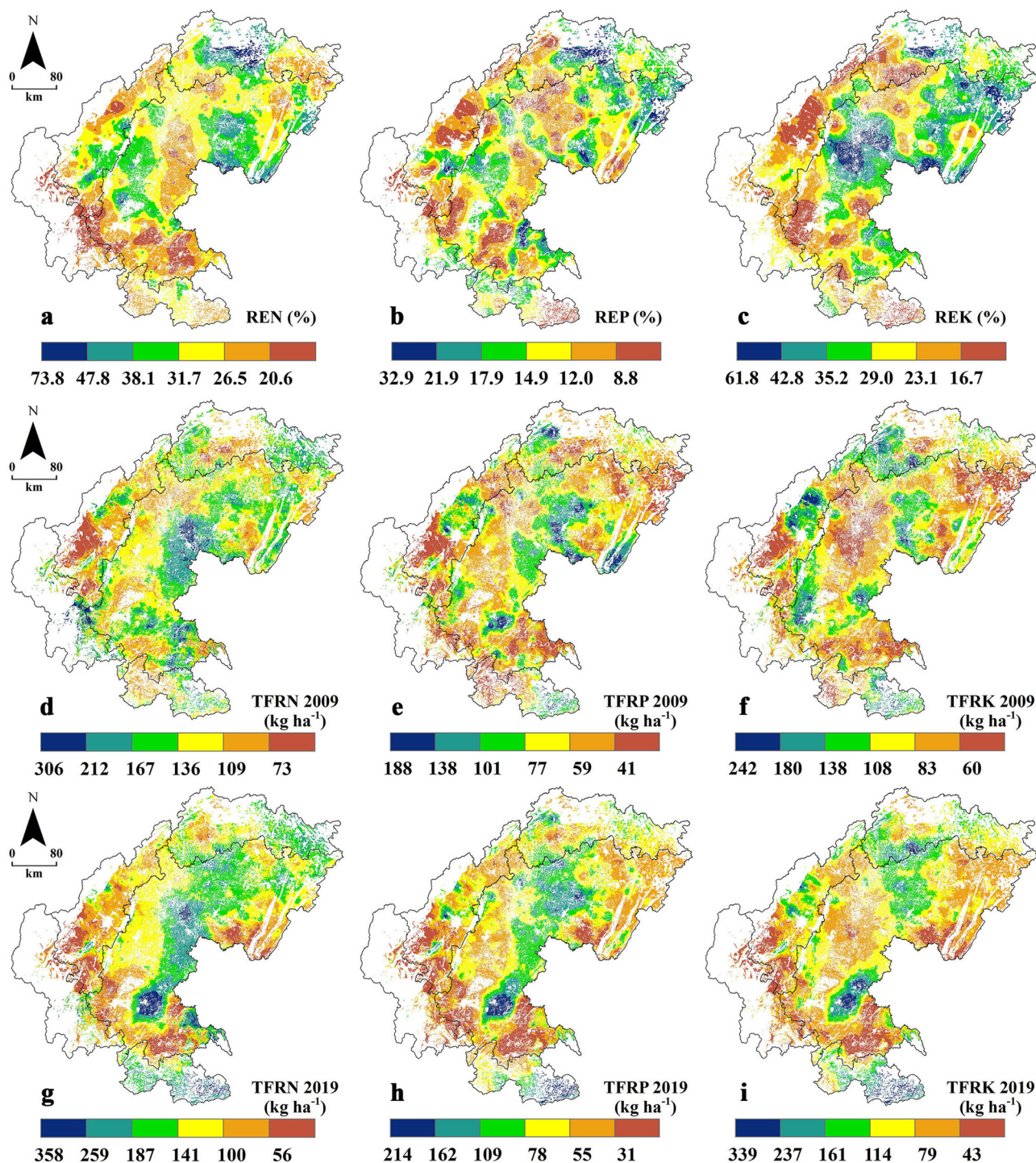
Fig. 3 Spatial distributions of rice fertilizer utilization efficiency and theoretical fertilizer rate in the Sichuan Basin, SW China. Spatial distributions of (**a**) nitrogen fertilizer utilization efficiency (REN), (**b**) phosphorus fertilizer utilization efficiency (REP) and (**c**) potassium fertilizer utilization efficiency (REK). Spatial distribution of (**d**) theoretical nitrogen fertilizer rate (TFRN), (**e**) theoretical phosphate fertilizer rate (TFRP), and (**f**) theoretical potassium fertilizer rate (TFRK) in 2009 and (**g**) TFRN, (**h**) TFRP, (**i**) TFRK in 2019.

TFRN, TFRP, and TFRK were 121.4 kg ha^{-1}, 60.9 kg ha^{-1}, and 87.4 kg ha^{-1} in 2019, respectively (Figs. 3 and 4, and Supplementary Table 10). In general, the nutrient demand of rice in the Sichuan Basin showed a decreasing trend from 2009 to 2019. In particular, the demand for nitrogen and phosphorus was significantly lower in the plains than in the hills and mountains. In spatial distribution, nutrient demand was relatively low in the western part of the plains, along the Minjiang River-Yangtze River, and in the eastern part of the hills; and relatively high in the north-central part of the hills and in the mountains.

The NBRN, NBRP, and NBRK were 0.32, 0.14, and −0.29, respectively, in 2009; the NBRN, NBRP, and NBRK were 0.44, 0.24, and −0.15, respectively, in 2019 (Figs. 4 and 5, and Supplementary Table 11). The trend of nitrogen and phosphorus excess is increasing, while the trend of potassium deficiency is reversed from 2009 to 2019. Notably, the nutrient balance has an
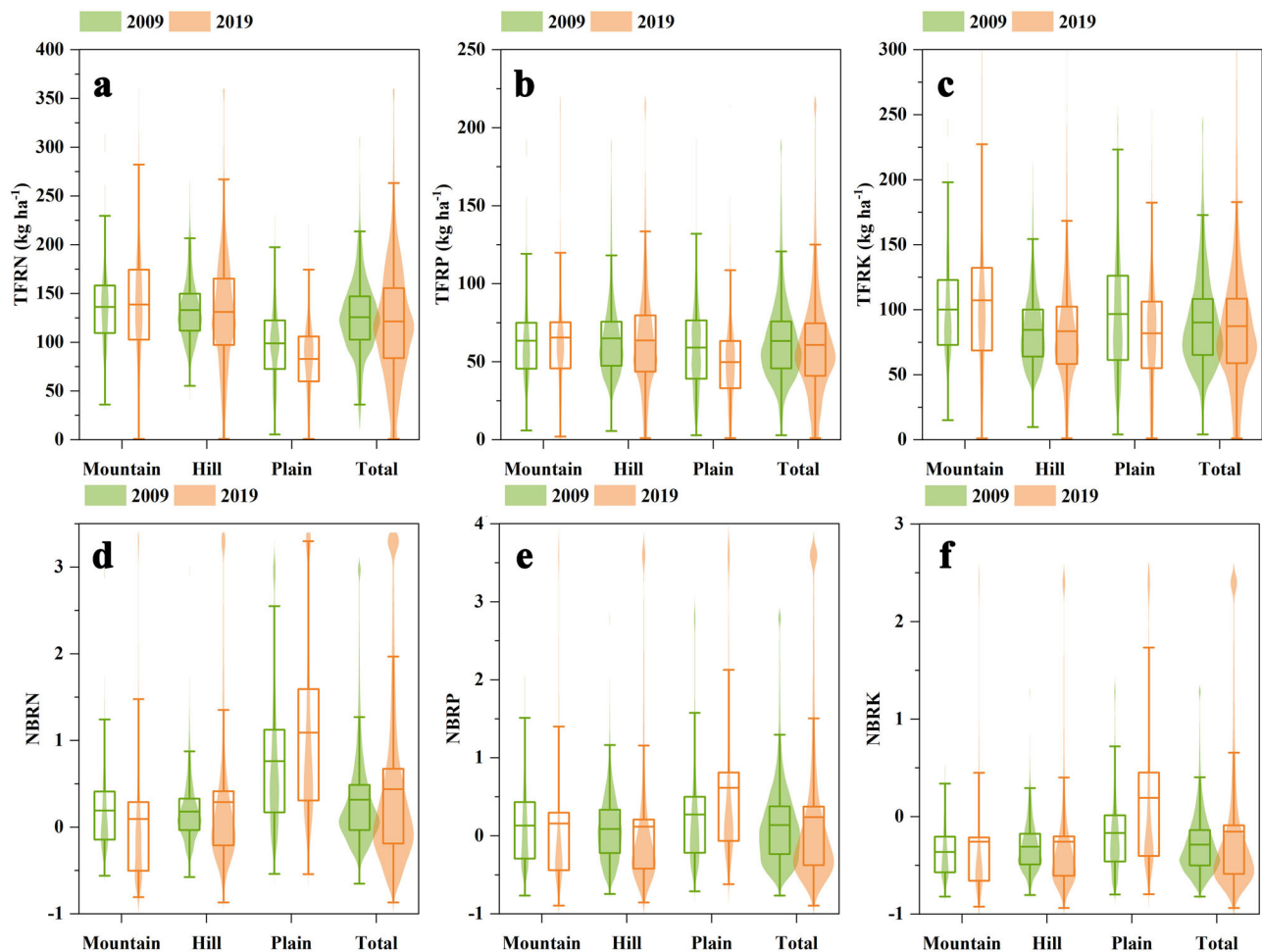
Fig. 4 Statistics chart of rice theoretical fertilizer rate and nutrient balance ratio in Sichuan Basin, SW China. Fiddle plots of (**a**) TFRN, (**b**) TFRP, (**c**) TFRK, (**d**) NBRN, (**e**) NBRP, and (**f**) NBRK for all grids (4.87×10^6). Boxes represent interquartile range with the mean value as the bold line, whiskers represent 1.5 interquartile range, and the outer border represents the data distribution. Positive nutrient balance ratios indicate excessive nutrient inputs, zero nutrient balance ratios indicate balanced nutrient inputs, and negative nutrient balance ratios indicate insufficient nutrient inputs.

obviously spatial heterogeneity in the Sichuan Basin. In the plains, there is a general excess of nitrogen and phosphorus, while there is an excess of potassium in the south-west and insufficient potassium in the north-east. In the hills, the nutrient balances are bifurcated, with nitrogen insufficient in the center and excessive in the surroundings, phosphorus insufficient in the north-central part and excessive in the south and east, and potassium generally insufficient except along the Yangtze River. Meanwhile, the area of nutrient insufficiency in the hills shows an expanding trend from 2009 to 2019. In the mountains, nutrient excesses are mainly concentrated in the west, while nutrients are generally insufficient in the north and south.

Farmland nutrient sustainability classification and characteristics. SPSS Modeler was used to build a Self-organizing feature map (SOFM) model for identifying and zoning farmland nutrient sustainability. Here, we used 2019 NBRN, NBRP, and NBRK as input parameters to accurately classify 4.87 million grids in the Sichuan Basin (Supplementary Table 12). Silhouette measure of cohesion and separation of the SOFM model is 0.46, indicating that the clustering results were reliable. Using SOFM clustering, we can divide the study area into three categories (Table 2, Supplementary Table 13, Supplementary Table 14 and Supplementary Fig. 7): the first category is the Sustainable Zone (SZ), accounting for 44.6% of the study area. This zone has a slight excess of nitrogen, a balanced phosphorus and

a slight deficiency of potassium. Meanwhile, the FIY was 2.2 t ha^{-1}, with FCR of 26.3%, generally achieving a sustainable use of nutrient resources. The second category is the Excess Risk Zone (EZ), accounting for 19.4% of the study area. The nutrient balance ratio of nitrogen, phosphorus and potassium in this zone was greater than 1, especially nitrogen and phosphorus were almost doubled. Due to the highest soil nutrient content (except potassium) in this zone, coupled with the highest fertilizer inputs, the FCR was only 10.9% and the FIY was only 0.9 t ha^{-1}. Excess nitrogen and phosphorus led to a significant reduction in the nutrient use efficiency of rice and serious environmental risks. The third category is the Degradation Risk Zone (DZ), accounting for 36.0% of the study area. The nutrient balance ratio of nitrogen, phosphorus and potassium in this zone is negative, especially potassium is apparently deficient. Due to the lowest soil nutrient content (except potassium), coupled with the lowest fertilizer inputs, rice in this zone had the strongest fertilizer response, with FIY of 3.3 t ha^{-1} and FCR of 38.1%. However, inadequate fertilizer inputs could lead to soil nutrient depletion, thereby increasing the risk of soil degradation. Furthermore, the standard deviation of FIY was significantly higher in the degradation risk zone than in the other zones, indicating that inadequate nutrient inputs negatively affected rice yield stability.

In general, Sichuan Basin is facing the serious problems of excessive and degraded farmland nutrients, with degradation risk zones accounting for about 36% of the total area and excess risk
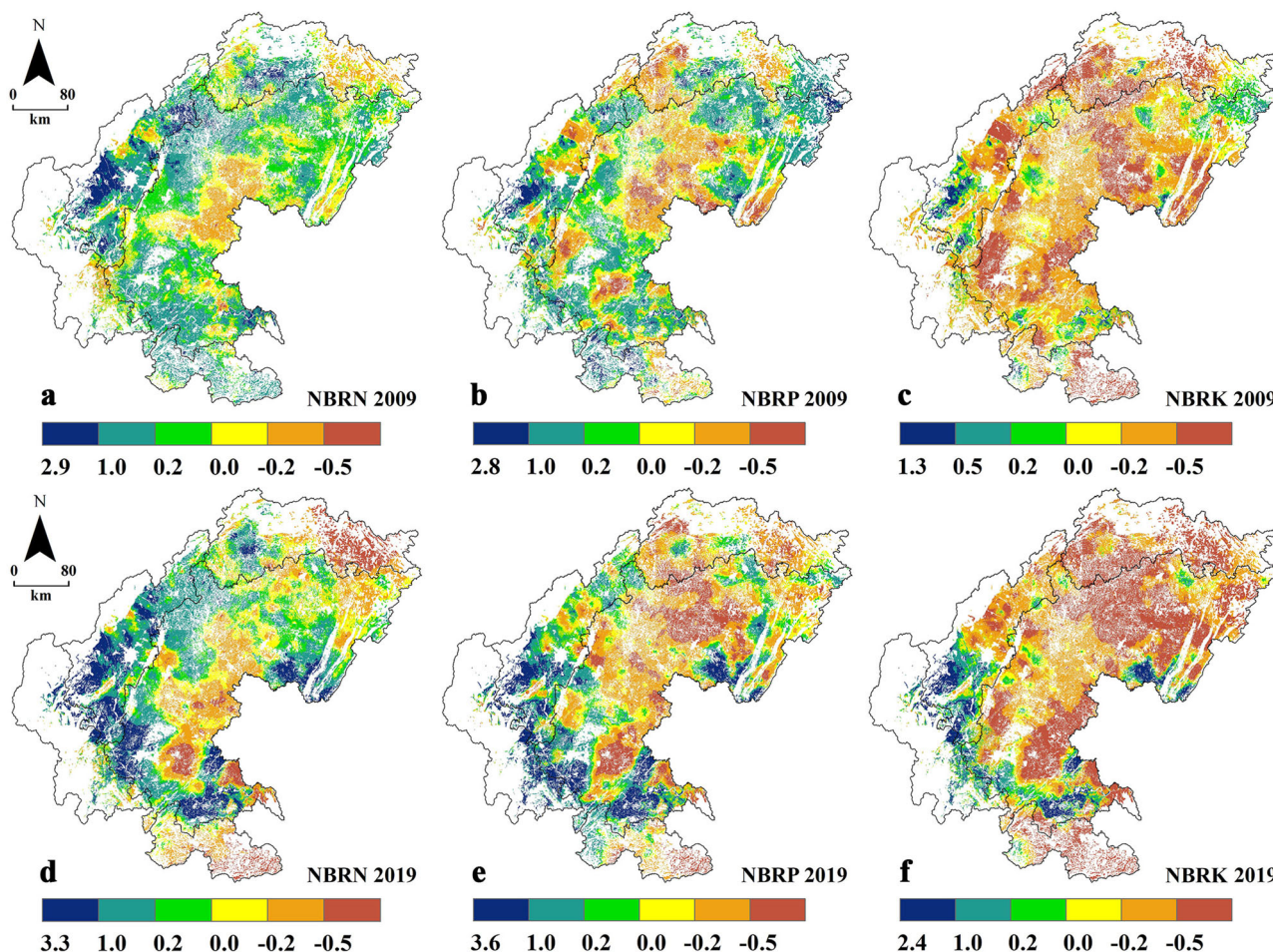
Fig. 5 Spatial distributions of rice nutrient balance ratio in the Sichuan Basin, SW China. Spatial distributions of NBRN, NBRP, and NBRK in 2009 (**a–c**) and 2019 (**d–f**). Positive nutrient balance ratios indicate excessive nutrient inputs, zero nutrient balance ratios indicate balanced nutrient inputs, and negative nutrient balance ratios indicate insufficient nutrient inputs.

Table 2 Statistics on zoning results of farmland nutrient sustainability.

Type	Area (10³ ha⁻¹)	Nutrient balance ratio	Mean	Min	Max	S.D.
Sustainable zone	1420.4	NBRN	0.33	−0.54	3.30	0.42
		NBRP	0.04	−0.80	2.43	0.36
		NBRK	−0.32	−0.87	1.75	0.24
Excess risk zone	1761.3	NBRN	1.96	−0.35	3.30	1.06
		NBRP	1.85	−0.44	3.60	1.23
		NBRK	1.01	−0.75	2.40	0.95
Degradation risk zone	766.6	NBRN	−0.27	−0.87	0.62	0.24
		NBRP	−0.41	−0.89	0.67	0.19
		NBRK	−0.60	−0.94	0.20	0.15

zones accounting for about 19% of the total area. Figure 6 shows that the nutrient degradation zones are mainly distributed in the central and northern hills, and the northern and southern mountains. The nutrient excess zones are mainly distributed in the south-western plains, along the Minjiang-Yangtze River and in the eastern part of the hills. The nutrient sustainable zones are mainly distributed in the western, southwestern and northeastern hills, central and northern plains. The plains have the highest farmland nutrient sustainability, but also the highest risk of nutrient excess, with 58% and 37% of sustainable and excess areas, respectively. The hills have medium farmland nutrient sustainability, mainly at risk of nutrient degradation, with 14% and 42% of excess and degraded areas, respectively. Mountains

have the lowest farmland nutrient sustainability, with 53% of the area at risk of nutrient degradation.

Impact factors on rice yield and nutrient balance. Pearson correlation analysis showed that natural and socio-economic factors influenced rice yield and nutrient balance differently, with a general consistency across different regions (Fig. 7). Socio-economic factors had little effect on rice yield and nutrient balance overall. The economy and population had a slightly negative effect on yield in areas of excess risk and a slightly positive effect on yield in areas of degradation risk. The closer to towns, roads and rivers, the higher the rice yield. This may be due to the flat
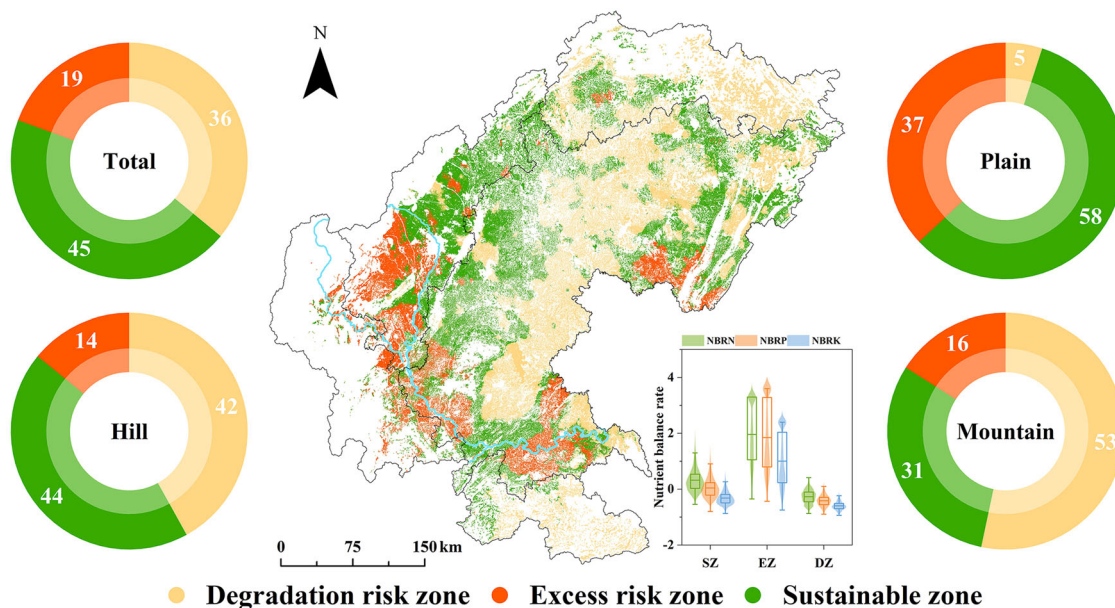
Fig. 6 Spatial distribution of farmland nutrient sustainability zones in Sichuan Basin, SW China. The pie charts represent the proportion (%) of the area of the sustainable zone (green), the excess risk zone (red) and the degradation risk zone (yellow) for the different regions. The fiddle chart represents the statistics of NBRN, NBRP, and NBRK for sustainable zone, excess risk zone, and degradation risk zone. Boxes represent interquartile range with the mean value as the bold line, whiskers represent 1.5 interquartile range, and the outer border represents the data distribution. Positive nutrient balance ratios indicate excessive nutrient inputs, zero nutrient balance ratios indicate balanced nutrient inputs, and negative nutrient balance ratios indicate insufficient nutrient inputs.

topography, high soil nutrients and better infrastructure near these areas, resulting in higher rice yields. Precipitation had a significant positive effect on yield, while temperature and terrain had a negative effect. The lower the slope and the lower the altitude, the higher the rice yield. The study area is close to the Tibetan Plateau in the northwest and belongs to the southeastern monsoon climate zone, so the eastern and southern parts of the study area have better thermal and hydrological conditions, which is beneficial to the increase of rice yield. Soil pH, available phosphorus, and available potassium had a positive effect on rice yield, while soil organic matter and total nitrogen had a negative effect. In general, soil nutrients had a negative effect on nutrient balance, which indicated that the improvement of basal soil fertility could reduce fertilizer inputs.

Discussion

Due to the spatial heterogeneity of various factors affecting rice yield, the yield prediction results of traditional global models will be biased[73]. The GWRK model in this paper reliably solves the problem of spatial non-stationarity of the predictor variables. The results of an empirical study in a main rice-growing areas of southwest China are consistent with related studies[74], proving the reliability of this method. In general, the accuracy of rice yield prediction has generally reached a high level[40,75], and the prediction accuracy in hills and plains was obviously higher than that in mountains. On the one hand, due to the small number and uneven spatial distribution of fertilizer response experiments in mountainous areas, the prediction accuracy of the model decreased. On the other hand, relevant studies have shown that water and low-temperature stress can lead to a decline in the accuracy of crop yield simulation[76]. The mountainous areas of Sichuan Basin are severely affected by seasonal drought and extreme temperatures[77], which may also be an important reason for the lack of simulation accuracy. Meanwhile, due to the lack of consideration of factors such as crop varieties and pests[78], the

uncertainty of the prediction results was increased to some extent. Notably, the method in this paper bridges the gap between microscopic field experiments and macroscopic spatial simulations, which has advantages in accurately simulating the response of rice yield to fertilizer inputs under different soil nutrient conditions. In contrast, prediction methods such as remote sensing have the advantage of accuracy, but cannot effectively explain the reasons for crop yield variation, especially the interactions between crop yield, soil nutrients and fertilizer inputs[79]. At present, field experiments have attracted widespread attention and popularity around the world, providing a reliable source of the data required for the methodology of this paper[80,81]. This method can be applied more broadly in the future as more experimental data is available.

Rice yield is sensitive to changes in meteorological and soil factors in southwest China. From 2009 to 2019, we observed an increasing trend in both YS and YF in the Sichuan Basin. There were two main regions of YS improvement (Fig. 2): one is the eastern and southwestern part of the hills, where the spatial location of the YS improvement coincided with the increase in precipitation (Fig. 2, Supplementary Figs. 11 and 12, and Supplementary Table 19), so precipitation may be the dominant factor for the increase in YS in this area; the other is the plain, where the increase in soil nutrients was significantly higher than that of other regions, which may be the main reason for the improvement in YS. In addition, factors such as improved farmland management and atmospheric nitrogen deposition may also contributed to the increase in YS[82,83]. The change in YF was similar to that of YS, but the increase in YF was lower than that of YS due to a decrease in fertilizer rates (Fig. 2 and Supplementary Table 19). Significantly, the average content of soil organic matter in Sichuan Basin increased by 2.1 g/kg, but this change had a small impact on rice yield, indicating that soil organic matter may not be a limiting factor for rice growth in the study area. Nitrogen fertilizer increase will cause nutrient excesses, which provides valid evidence for enhanced control of nitrogen fertilizer use in
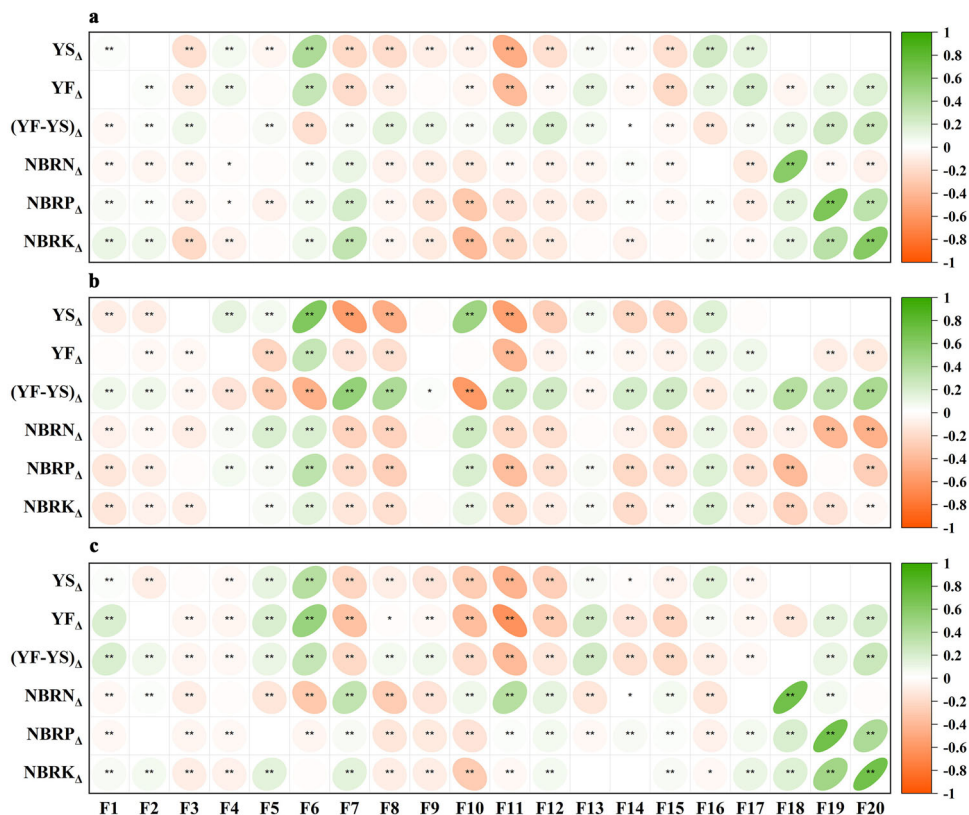
Fig. 7 Correlation plot of rice yield, nutrient balance ratio and the natural social factors in Sichuan Basin, SW China. Correlation analysis of (**a**) sustainable zone, (**b**) excess risk zone and (**c**) degradation risk zone. YS_Δ, YF_Δ, $(YF-YS)_\Delta$, $NBRN_\Delta$, $NBRP_\Delta$, and $NBRK_\Delta$ represent changes in YS, YF, FIY, NBRN, NBRP, and NBRK from 2009 to 2019. The horizontal coordinates indicate the change in gross domestic product (**F1**), population density (**F2**), annual mean precipitation (**F6**), annual mean temperature (**F7**), NDVI (**F12**), soil pH (**F13**), soil OM (**F14**), soil TN (**F15**), soil AP (**F16**), soil AK (**F17**), FRN (**F18**), FRP (**F19**), FRK (**F20**) from 2009 to 2019, and distance from cities (**F3**), distance from roads (**F4**), distance from rivers (**F5**), altitude (**F8**), slope (**F9**), longitude (**F10**), latitude (**F11**). Positive (negative) values indicate a positive (negative) correlation between indicators. Lighter colors indicate smaller correlation coefficients and lower correlations. (*****) indicates that the correlation reaches a significant level ($p \leq 0.05$), (******) indicates that the correlation reaches an extreme significant level ($p \leq 0.01$).

the main rice-growing areas of southwest China[84,85]. Soil available phosphorus had a positive effect on rice yield, but the increase of soil phosphorus also causes phosphorus excess in some regions (excess risk zone). Soil available potassium increases rice yield while contributing to the potassium balance. Since potassium deficiency is widespread in the Sichuan Basin (Supplementary Table 19), increasing potassium inputs may be a key component of nutrient sustainability in the main rice-growing regions.

The degradation risk zone and the excess risk zone should be the critical areas for the farmland nutrient resource regulation in the Sichuan Basin. *Degradation risk zone*: increasing organic and potash fertilizer inputs, appropriate supplementation of phosphorus fertilizer and improving soil nutrient levels will be the focus of future nutrient management. Over the last 10 years, the average nitrogen, phosphorus, and potassium fertilizer inputs in the degradation risk zone decreased by 26 kg ha^{-1}, 16 kg ha^{-1}, and 10 kg ha^{-1}, respectively, and the phosphorus and potassium fertilizer inputs were significantly lower than those in other regions (Supplementary Table 14); soil organic matter, available phosphorus and available potassium decreased by 2.2 g kg^{-1}, 10.8 mg kg^{-1} and 43 mg kg^{-1}, respectively. Except for potassium, soil nutrient levels in the degradation risk zone were already the lowest in the study area (Supplementary Table 14). *Excess risk zone*: Strict control of nitrogen and phosphorus inputs and moderate use of potassium fertilizer to maintain soil nutrients is

the key to nutrient regulation. Soil nutrients are highest in this area, but high fertilizer inputs cause serious excesses of nitrogen and phosphorus (Supplementary Table 14). Importantly, the excess risk zones have the potential to reduce at least 20,000 t of nitrogen and 9000 t of phosphorus per year (20% reduction), based on the reality of a 1–2 times excess of nitrogen and phosphorus. *Sustainable zone*: nutrient regulation will focus on moderately reducing nitrogen fertilizer and increasing potassium. The NBRN of this zone is 0.33 (Table 3), indicating that this area is still at risk of excessive nitrogen.

Conclusions
Optimal management of farmland nutrient resources is an important foundation for sustainable agriculture in China. Based on the idea of "nutrient supply change—crop yield response— nutrient sustainable zoning", we propose a new assessment framework for farmland nutrient sustainability. First, the GWRK model has reliability and accuracy, but there were spatial differences in the prediction accuracy, with the accuracy of the model in the hills and plains being significantly higher than that in the mountains. Second, we found that fertilizer input made an important contribution to the long-term growth and stability of rice yield in southwest China. Over the past 10 years, fertilization has increased rice yield by 2.3–2.4 t ha^{-1} (FCR: 27–29%) and improved rice yield stability. However, the nutrient use efficiency

Table 3 Theoretical semi-variogram models and corresponding parameters of soil properties and fertilizer rates.

Year	Variable	Model	Nugget (C_0)	Sill ($C_0 + C$)	Range (km)	$C_0/(C_0 + C)$ (%)	R^2	Residual
2009	Soil OM (g kg^{-1})	E	0.17	0.31	61.9	54.8	0.846	2.289×10^{-3}
	Soil pH	E	0.73	1.48	139	49.3	0.985	9.794×10^{-3}
	Soil AP (mg kg^{-1})	E	0.48	0.67	14	71.6	0.933	2.173×10^{-3}
	Soil AK (mg kg^{-1})	E	0.17	0.24	40.3	70.8	0.73	1.492×10^{-3}
	FRN (N; kg ha^{-1})	S	0.03	0.09	9.3	33.3	0.84	7.579×10^{-4}
	FRP (P$_2$O$_5$; kg ha^{-1})	G	0.08	0.14	11.7	57.1	0.743	1.717×10^{-3}
	FRK (K$_2$O; kg ha^{-1})	E	0.06	0.12	12.1	50.0	0.863	3.054×10^{-4}
2019	Soil OM (g kg^{-1})	E	0.13	0.27	34.7	48.1	0.966	3.922×10^{-4}
	Soil pH	S	0.91	1.83	22.8	49.7	0.994	1.23×10^{-2}
	Soil AP (mg kg^{-1})	E	0.86	1.37	12.4	62.8	0.912	1.56×10^{-2}
	Soil AK (mg kg^{-1})	E	0.19	0.3	47.5	63.3	0.978	1.195×10^{-3}
	FRN (N; kg ha^{-1})	E	0.32	0.53	67.7	60.4	0.894	4.639×10^{-3}
	FRP (P$_2$O$_5$; kg ha^{-1})	E	0.23	0.38	16.8	60.5	0.718	3.169×10^{-3}
	FRK (K$_2$O; kg ha^{-1})	E	0.3	0.59	17.7	50.8	0.926	3.739×10^{-3}

of farmland in the study area showed a downward trend, with the FCR decreasing from 29.3% in 2009 to 27.5% in 2019. Third, the main rice-growing areas in southwest China face serious problems of excessive and degraded farmland nutrients. The nutrient imbalance is mainly characterized by excess nitrogen and phosphorus and insufficient potassium. The NBRN, NBRP, and NBRK were 0.32, 0.14, and −0.29, respectively, in 2009; the NBRN, NBRP, and NBRK were 0.44, 0.24, and −0.15, respectively, in 2019. Finally, The Sichuan Basin is divided into three farmland nutrient sustainability zones: the degradation risk zone, the excess risk zone, and the sustainable zone, accounting for 36.0%, 19.4%, and 44.6% of the total area, respectively. Controlling nitrogen and phosphorus inputs and increasing soil organic matter and potassium are key to future nutrient regulation of farmland in the Sichuan Basin. This paper provides a new approach to the optimal allocation of farmland nutrient resources under the dual objective constraints of food security and ecological security.

Methods
Study area. The Sichuan Basin is located in the upper reaches of the Yangtze River in southwest China (28°00′–31°59′ N, 102°47′–107°30′ E), which includes 124 counties in 17 cities, covering an area of 180,900 km^2 (Fig. 8). This region belongs to the humid subtropical climate zone, with an average annual temperature of 16–18 °C, an accumulated temperature of 4000–6000 °C, and a frost-free period of 230–340 days. The annual sunshine time is short, with only 1000–1400 h of annual sunshine, which is 600–800 h less than the annual sunshine in the lower reaches of the Yangtze River Basin at the same latitude, and it is the region with the least sunshine in China. Annual precipitation is 900–1200 mm in most areas, with more than 50% concentrated in the summer. As the Sichuan Basin is located in the transition zone between the Qinghai–Tibet Plateau and the eastern plains, the landform types are complex and diverse, with an altitude of 250–3000 m, mainly including three types of landforms: plain, hill, and mountain. The alluvial plain (Chengdu plain) is distributed in the western part of the basin, with a relative height difference of less than 20 m, and the surface is covered with fertile moisture soil. The hills are distributed in the central part of the basin; the altitude is generally 250–600 m, and the relative height is 20–200 m. Cretaceous-Jurassic purple sandstone shale is exposed on the surface, making this the most concentrated area of purple soil in China. The mountains are distributed around the edge of the basin; they are mainly low and medium mountains with an altitude of 1000–3000 m, and the soil is mainly zonal yellow soil.

The Sichuan Basin includes the most developed urban agglomeration in western China, Chengdu-Chongqing, and is also a key functional area for food supply and ecological protection in the Yangtze River Economic Belt. In 2020, the resident population of the Sichuan Basin was 75.7 million; the GDP exceeded 4.5 trillion CNY; and the total cultivated area was 5.88 million ha. The rice yield exceeded 14.2 million tons, accounting for about 54% of the total grain yield. The proportion of rice planting area in the plain, hill, and mountain areas of the Sichuan Basin is 21%, 61%, and 18%, respectively. However, due to rapid urbanization and population growth in the Sichuan Basin, the excessive and unbalanced inputs of chemical fertilizer to farmland have resulted in low regional fertilizer utilization efficiency. Currently, the total consumption of chemical fertilizers in this region exceeds 1.61 million tons (76.4% of Sichuan Province), and the consumption per unit area exceeds 332 kg ha^{-1} (N exceeds 143 kg ha^{-1}), which is significantly higher than the international level[86]. The risk of agricultural non-point source pollution in Sichuan Basin is already moderate[87]. Therefore, it is fundamental to regulate and optimize regional farmland nutrient resources.

"3414" fertilizer field experiment. The field experiment data were collected from the *Soil Testing and Formulated Fertilization Project* (STFF) in Sichuan Province. The fertilizer response field experiments included 1182 rice experiments (plain: 251, hill: 708, mountain: 223) from 2009 to 2019 (Fig. 9a). These experiments used the "3414" design scheme with three factors (nitrogen, phosphorus, and potassium), four fertilization levels for each factor, and a total of 14 experimental treatments (Supplementary Table 15)[88]. The meaning of the four fertilization levels: level 0 means no fertilization, level 2 refers to the representative fertilization rate of the experiment area (N, P$_2$O$_5$, and K$_2$O), level 1 = level 2 × 0.5 (this level represents insufficient fertilization), level 3 = level 2 × 1.5 (this level represents excessive fertilization). The average fertilizer rates of N, P$_2$O$_5$, and K$_2$O at level 2 in this study were 151.5, 75.0, and 75.3 kg ha^{-1}, respectively. The fertilizer rate ranges of N, P$_2$O$_5$, and K$_2$O were 45–390 kg ha^{-1}, 27–180 kg ha^{-1}, and 15–300 kg ha^{-1}, respectively (Supplementary Table 16 and Supplementary Fig. 9). The 14 experimental treatments were (1) N$_0$P$_0$K$_0$, (2) N$_0$P$_2$K$_2$, (3) N$_1$P$_2$K$_2$, (4) N$_2$P$_0$K$_2$, (5) N$_2$P$_1$K$_2$, (6) N$_2$P$_2$K$_2$, (7) N$_2$P$_3$K$_2$, (8) N$_2$P$_2$K$_0$, (9) N$_2$P$_2$K$_1$, (10) N$_2$P$_2$K$_3$, (11) N$_3$P$_2$K$_2$, (12) N$_1$P$_1$K$_2$, (13) N$_1$P$_2$K$_1$, and (14) N$_2$P$_1$K$_1$. Yield data (kg ha^{-1}) of each experimental treatment were recorded after rice harvest. In addition, indicators of soil physical and chemical properties such as organic matter (OM),
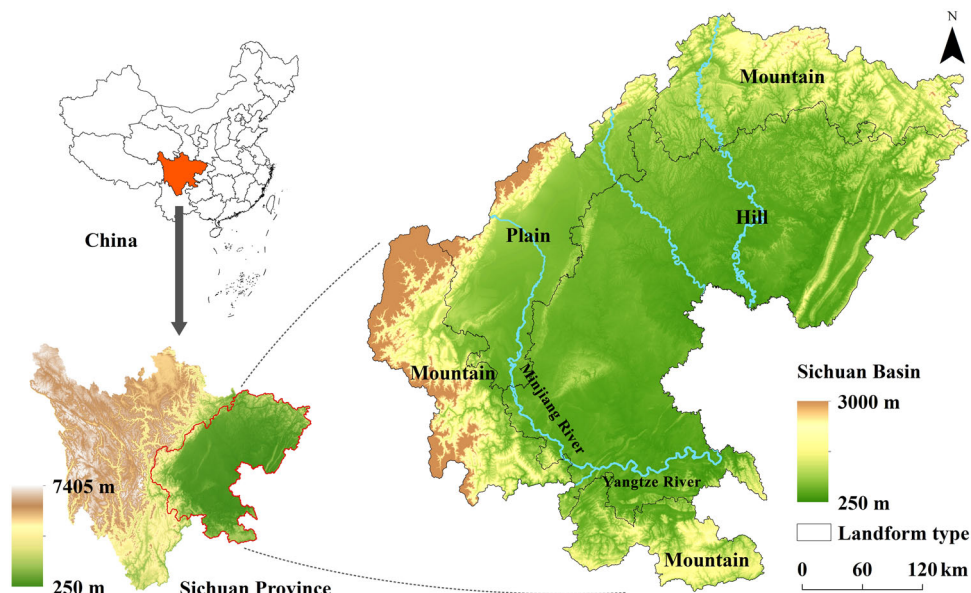
Fig. 8 Location and landform type of the study area in Sichuan Basin, SW China. The color fills in the figure represent the altitude (m) of the study area. Black lines divide the study area into plains, hills and mountains. Blue lines represent major rivers.
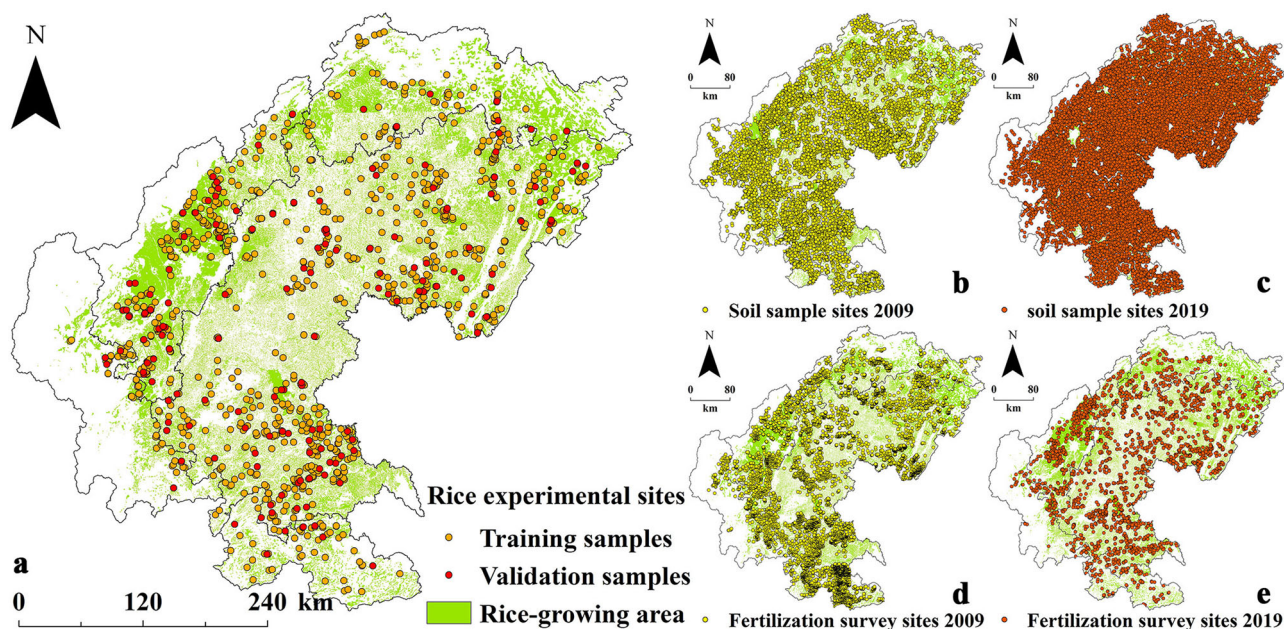

Fig. 9 Distribution of rice field experiments and survey sites in Sichuan Basin, SW China. a Rice fertilizer response field experiments in 2009-2019. **b** Soil sample sites in 2009. **c** Soil sample sites in 2019. **d** Fertilizer survey sites in 2009. **e** Fertilizer survey sites in 2019.

pH, available phosphorus (AP), and available potassium (AK) were tested at each field experimental site.

Soil properties and fertilizer rates. The soil data were obtained from the *STFF* and the *Cultivated Land Quality Monitoring Project* in Sichuan Province. The soil data (OM, pH, AP, and AK) included 2 years: 20,798 soil sampling points from 2009 and 17,737 soil sampling points from 2019. Rice fertilizer rates were obtained from 3918 fertilization survey points from 2009 and 3344 fertilization survey points from 2019 (Fig. 9), including nitrogen fertilizer rate (FRN), phosphorus fertilizer rate (FRP) and potassium fertilizer rate (FRK). In this paper, we used geostatistical methods to estimate the spatial distribution of soil properties and fertilizer rates[89,90]. The semi-variance function is

the key to geostatistical analysis, reflecting the degree of the spatial autocorrelation of observations at different distances. The model can be expressed as

$$\gamma(h) = \frac{1}{2N(h)} \sum_{i=1}^{N(h)} \left[Z(x_i) - Z(x_i + h) \right]^2 \qquad (1)$$

where $\gamma(h)$ refers to the semi-variance function; h refers to the step size; $N(h)$ refers to the logarithm of the observed sample points s, and $Z(x_i)$ and $Z(x_i + h)$ refer to the measured values of the variable $Z(x)$ at the spatial positions x_i and $x_i + h$, respectively.

We used GS+ software for the geostatistical analysis of soil properties and fertilizer quantities in the Sichuan Basin. Table 3 shows the fitting results of the semi-variance model. The semi-variance function models of the study area include the Gaussian

model, the exponential model, and the spherical model. The seven factors in 2009 and 2019 had obvious spatial autocorrelation, and the range was generally greater than 10 km. Furthermore, high R^2 and low residuals indicated that the geostatistical methods were reliable in estimating the spatial distribution of soil and fertilizer factors. The process of geostatistical analysis of soils and fertilizers is presented in Supplementary Tables 17, 18 and Supplementary Fig. 10.

Meteorological, vegetation and terrain factors. The datasets of land use and cover, digital elevation model, normalized difference vegetation index in rice maturity stage (NDVI), annual mean precipitation (PRE), annual mean temperature (TEM), roads, rivers, and administrative districts were provided by the Data Center for Resources and Environmental Sciences, Chinese Academy of Sciences (RESDC)[91–94]. Socio-economic data were collected from the *Statistical Yearbook* of Sichuan Province and the *Statistical Yearbook* of various counties (2009 and 2019). Spatial distribution of population (1×1 km) and GDP (1×1 km) data also from RESDC. The spatial resolution of the raster data was uniform, 30×30 m (Supplementary Figs. 12 and 13).

Rice yield simulation under different nutrient conditions. GWR is a typical local spatial regression model, which decomposes global parameters into local parameters for estimation, and considers the relationship of non-stationarity when estimating the parameters of each spatial location point[95]. The GWR model is not only suitable for capturing the local variability of crop yields, but it also clearly explains the effects of environmental variables[96]. To further reduce the error in crop yield prediction, scholars have proposed the GWRK method, which combines GWR and kriging to quantify uncertainty in yield prediction results[97]. In this method, ordinary kriging (OK) interpolation is performed on the residuals obtained from the GWR local model fitting, and then added to the GWR fitting results.

Crop soil-based yield (YS) and fertilized yield (YF) can effectively reflect the contribution of farmland inherent soil productivity and fertilization for rice yield, respectively[98]. Here, using 1027 field experiments (plain: 213, hill: 611, mountain: 203) as training samples (Fig. 9a), we established GWRK models to simulate the effects of soil and fertilizer nutrient supply on YS and YF of rice. YS refers to rice yield without fertilization in the current year, expressed as the yield of treatment 1 ($N_0P_0K_0$) of the "3414" experiment[88]. The YS is important for two reasons: firstly, it shows the spatial distribution of rice yield reduction under the hypothetical condition of no fertilizer use; and secondly, the FIY (YF-YS) provides the possibility to calculate the theoretical fertilizer requirement of rice in order to assess the nutrient balance. The independent variables (explanatory variables) corresponding to the YS model include 9 environmental factors: soil OM (X_1), pH (X_2), soil AP (X_3), soil AK (X_4), PRE (X_5), TEM (X_6), NDVI (X_7), altitude (X8), and slope (X_9).

YF refers to rice yield under normal fertilization conditions (representative fertilization rate and cultivation management of local farmers). Since YF significantly depends on YS[98], we adopted the RYC as the dependent variable fitting model to improve the prediction accuracy, which is expressed as the ratio of the yield of treatment 1 and treatment 6 ($N_0P_0K_0/N_2P_2K_2$) in the "3414" experiment. Based on the YS model, the RYC model adds 3 fertilization quantity factors: FRN (X_{10}), FRP (X_{11}), and FRK (X_{12}), increasing the number of independent variables to 12. Finally, YF is calculated on the basis of RYC and YS. FIY is used to express the increase in rice yield due to fertilizer application by subtracting the soil base yield from the fertilizer applied yield; FCR was used to measure the contribution of fertilizer to rice

yield[99]. The model can be expressed as[100]

$$YS_i(\mu_i, \nu_i) = \beta_0(\mu_i, \nu_i) + \sum_k \beta_k(\mu_i, \nu_i)X_{ik} + \varepsilon_i, X_k = X_1, X_2, \cdots, X_9 \tag{2}$$

$$RYC_i(\mu_i, \nu_i) = \beta_0(\mu_i, \nu_i) + \sum_k \beta_k(\mu_i, \nu_i)X_{ik} + \varepsilon_i, X_k = X_1, X_2, \cdots, X_{12} \tag{3}$$

$$YF_i = YS_i/RYC_i \tag{4}$$

$$FIY_i = YF_i - YS_i \tag{5}$$

$$FCR_i = (YF_i - YS_i)/YF_i \times 100\% \tag{6}$$

where YS_i, RYC_i, YF_i, FIY_i, and FCR_i refer to the soil-based yield, the RYC, the fertilized yield, the FIY and the FCR of point i, respectively; (μ_i, ν_i) refers to the spatial coordinates of point i; β_0 refers to the intercept of point i; X_{ik} refers to the value of the explanatory variable of number k at point i; β_k refers to the regression coefficient of the explanatory variable of number k; and ε_i is the residual error of the GWR model after fitting in point i, which is calculated with interpolation using the OK method (Formula 1).

In order to evaluate the simulation accuracy of the GWRK model, we randomly selected 155 field experiments as verification samples to calculate the error between the actual yield and the predicted yield (Fig. 9a). The corresponding evaluation indicators and their formulas are as follows:

$$ME = 1/n\sum_{i=1}^n \{z(x_i) - z'(x_i)\} \tag{7}$$

$$MAE = 1/n\sum_{i=1}^n \{|z(x_i) - z'(x_i)|\} \tag{8}$$

$$RMSE = \sqrt{1/n\sum_{i=1}^n \{z(x_i) - z'(x_i)\}^2} \tag{9}$$

$$SMAPE = 1/n\sum_{i=1}^n \{(2 \times |z(x_i) - z'(x_i)|)/(|z(x_i)| + |z'(x_i)|)\} \times 100\% \tag{10}$$

where ME, MAE, RMSE, and SMAPE refer to the mean error, the mean absolute error, the root means square error, the mean relative error, and the symmetric mean absolute percentage error, respectively; $z'(x_i)$ refers to the predicted value of sample i; $z(x_i)$ refers to the actual observed value of sample i; and n refers to the number of samples. The smaller the MAE, RMSE, and SMAPE values are, the smaller the error and the higher the simulation accuracy are.

In this paper, we use the OAT (one-at-a-time) method to analyze the sensitivity of rice yield model parameters. Since topographic indicators change very little, we focus on analyzing the sensitivity of meteorological, vegetation, soil, and fertilizer parameters. The OAT method increases or decreases the value of only 1 parameter in the database by 10% each time, and then calculates the RSI[101]. The calculation formula is as follows

$$RSI = \left| \frac{[y(x + \Delta x) - y(x)]/y(x)}{\Delta x/x} \right| \tag{11}$$

where x refers to the value of a parameter in the model parameters; Δx is the amount of change in that parameter; $y(x)$ and $y(x + \Delta x)$ refer to the simulated output values (YS and RYC) before and after the parameter change, respectively. Higher values of RSI indicate that the parameter is more sensitive, and lower values are less sensitive.

Farmland nutrient sustainability assessment. Farmland nutrient sustainability is an important foundation for sustainable agriculture, but previous studies cannot accurately assess and identify
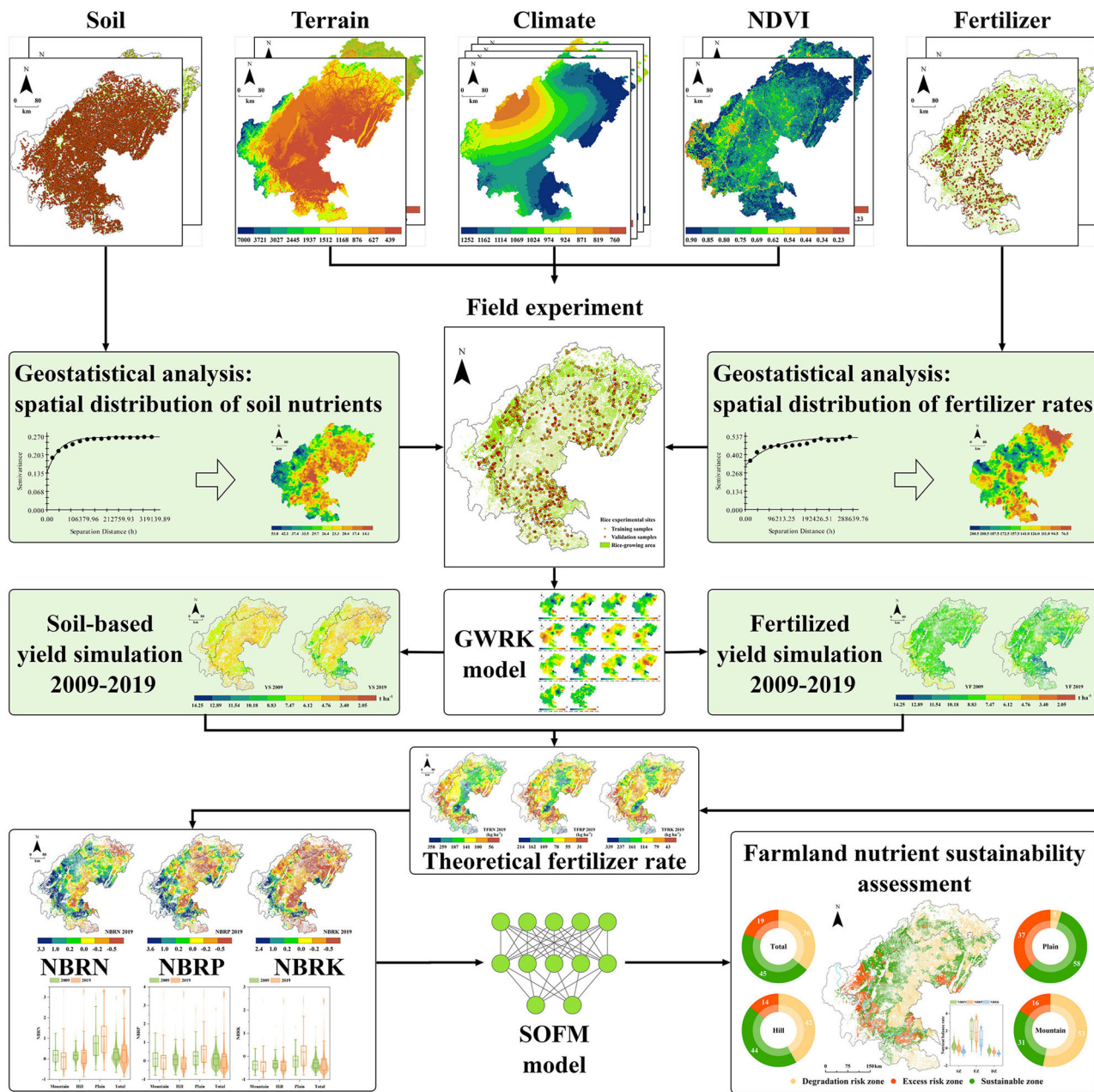
Fig. 10 Assessment framework for farmland nutrient sustainability. The rectangular boxes in the figure represent the main data types used in the study, the rounded rectangular boxes represent the main assessment steps, and the arrows represent the assessment process and sequence.

farmland nutrient sustainability in spatial locations[102,103]. Therefore, we propose a farmland nutrient sustainability assessment framework (Fig. 10) based on the interrelationships between soil, fertilizer and crop to achieve spatial optimization and precise management of farmland nutrient resources.

Calculation of nutrient uptake for 100 kg rice yield. Since the nutrient content of rice stems and leaves was not measured in the "3414" fertilizer field experiment, we used 103 rice fertilizer utilization efficiency field experiments in the Sichuan Basin to calculate nutrient uptake. There were five fertilizer treatments in the field experiments[104]: (1) nitrogen-phosphorus-potassium fertilizer; (2) phosphorus-potassium fertilizer; (3) nitrogen-potassium fertilizer; (4) nitrogen-phosphorus fertilizer; and (5) no fertilizer (CK). The experimental plots area for each treatment were 20–30 m^2 with three replications, arranged in random groups.

Fertilizer rates were representative fertilization levels of the experimental area. According to NY/T 2911 and relevant studies[105], the formula can be expressed as

$$NUTN = \left[Y_{SE} \times NCN_{SE} + Y_{SL} \times NCN_{SL} \times (1 - SR) \right] / Y_{SE} \times 100 \tag{12}$$

$$NUTP = \left[Y_{SE} \times NCP_{SE} + Y_{SL} \times NCP_{SL} \times (1 - SR) \right] / Y_{SE} \times 100 \tag{13}$$

$$NUTK = \left[Y_{SE} \times NCK_{SE} + Y_{SL} \times NCK_{SL} \times (1 - SR) \right] / Y_{SE} \times 100 \tag{14}$$

where *NUTN*, *NUTP*, and *NUTK* refer to nitrogen, phosphorus and potassium nutrient uptake (kg) for 100 kg rice yield, respectively. Y_{SE} and Y_{SL} refer to rice seed yield and stem-leaf yield

(kg ha^{-1}) in experimental treatment 1, respectively; NCN_{SE} and NCN_{SL} refer to rice seed total nitrogen content (%) and stem-leaf total nitrogen content (%) in experimental treatment 1, respectively; NCP_{SE} and NCP_{SL} refer to rice seed total phosphorus content (%) and stem-leaf total phosphorus content (%) in experimental treatment 1, respectively; NCK_{SE} and NCK_{SL} refer to rice seed total potassium content (%) and stem-leaf total potassium content (%), respectively; SR refers to the rice straw return rate, which was 64% in Sichuan Basin according to the relevant study[106].

Calculation of rice fertilizer utilization efficiency. Rice fertilizer utilization was calculated using the subtraction method[107,108]. First, we calculated the fertilizer utilization efficiency of rice in 1182 "3414" field experiments in the Sichuan Basin. Second, the results of the fertilizer utilization efficiency calculation were analyzed by Geostatistics (Supplementary Fig. 5 and Supplementary Table 8). Finally, ArcGIS was used to generate spatial distribution maps of rice fertilizer utilization in the Sichuan Basin. The formula can be expressed as

$$REN = NUTN \times (Y_{NPK} - Y_{PK})/FerN \times 100 \quad (15)$$

$$REP = NUTP \times (Y_{NPK} - Y_{NK})/FerP \times 100 \quad (16)$$

$$REK = NUTK \times (Y_{NPK} - Y_{NP})/FerK \times 100 \quad (17)$$

where REN, REP, and REK refer to rice nitrogen, phosphorus and potassium fertilizer utilization efficiency (%), respectively. Y_{NPK} refers to the rice yield of "3414" experimental treatment 6 ($N_2P_2K_2$) with nitrogen, phosphorus and potassium fertilizers; Y_{PK} refers to the rice yield of "3414" experimental treatment 2 ($N_0P_2K_2$) without nitrogen fertilizers; Y_{NK} refers to the rice yield of "3414" experimental treatment 4 ($N_2P_0K_2$) without phosphate fertilizer; Y_{NP} refers to the rice yield of "3414" experimental treatment 8 ($N_2P_2K_0$) without potassium fertilizer; $FerN$, $FerP$, and $FerK$ refer to the nitrogen, phosphorus, and potassium fertilizer rates (2 levels) in the "3414" experiment, respectively.

Calculation of the theoretical nitrogen fertilizer rate. based on the nutrient balance method[109], the theoretical rate of nitrogen, phosphorus, and potassium fertilizer for rice was calculated using the predicted results of YS and YF. Then, the theoretical fertilizer rate was compared with the actual fertilizer rate to calculate the nutrient balance rates of nitrogen, phosphorus and potassium[110]. The calculation formulas can be expressed as

$$TFRN = [(YF - YS) \times NUTN]/(REN \times 100) \quad (18)$$

$$TFRP = [(YF - YS) \times NUTP]/(REP \times 100) \quad (19)$$

$$TFRK = [(YF - YS) \times NUTK]/(REK \times 100) \quad (20)$$

$$NBRN = (FRN - TFRN)/TFRN \times 100\% \quad (21)$$

$$NBRP = (FRP - TFRP)/TFRP \times 100\% \quad (22)$$

$$NBRK = (FRK - TFRK)/TFRK \times 100\% \quad (23)$$

where $TFRN$, $TFRP$, and $TFRK$ refer to the theoretical nitrogen fertilizer rate (kg ha^{-1}), theoretical phosphate fertilizer rate (kg ha^{-1}), and theoretical potassium fertilizer rate (kg ha^{-1}) in each grid, respectively; YS and YF refer to the soil-based yield and fertilized yield calculated in formula (2) and (4) in each grid, respectively. $NUTN$, $NUTP$, and $NUTK$ refer to nitrogen, phosphorus and potassium nutrient uptake (kg) for 100 kg rice yield, respectively. REN, REP, and REK refer to rice nitrogen, phosphorus and potassium fertilizer utilization efficiency (%) in each grid, respectively; $NBRN$, $NBRP$, and $NBRK$ refer to nitrogen,

phosphorus and potassium nutrient balance ratios in each grid, respectively ($NBR > 0$ indicates excessive nutrient inputs, $NBR = 0$ indicates balanced nutrient inputs, and $NBR < 0$ indicates insufficient nutrient inputs).

Nutrient sustainability assessment based on the SOFM model. SOFM is a type of unsupervised artificial neural network[111] that has been widely used in the clustering or partitioning work of geography and ecology[112,113]. Therefore, SOFM clustering was used to identify farmland nutrient sustainability in this paper. The NBRN, the NBRP and the NBRK are used as input nodes of the SOFM model. According to the SOFM clustering results, the nutrient sustainability zones such as nutrient excess, nutrient degradation, and nutrient sustainability were identified and classified. The SOFM network calculation process is as follows:

(1) Initialize the connection weights of n input nodes to output nodes and assign a random initial value w_{ij}. Meanwhile, set the initial neighborhood domain for each output node j.

(2) Normalize the input sample set. Then, select a sample from the sample set as the input vector and calculate the Euclidean distance, d_j, between the input vector and each output node j. The calculation formula is

$$d_j = \|X - W_j\| = \sqrt{\sum_{i=1}^{n}[x_i(t) - w_{ij}(t)]^2} \quad (24)$$

(3) The output node k with the minimum distance is selected as the winning node. Given a surrounding domain $S_k(t)$, update the weights of the winning node and of the nodes in its surrounding domain. The weight change is

$$\Delta w_{ij} = \eta(t)\left[x_i(t) - w_{ij}(t)\right], j \in S_k(t) \quad (25)$$

where η refers to a positive learning rate, decreasing with time.

(4) Repeat steps 2–3 until the number of iterations is met.

(5) Input all samples for calculation; finally, according to the clustering results, classify the storage.

Data availability

Full details of all datasets used in the study are further elaborated in the Supplementary Information and available at Dryad (https://doi.org/10.5061/dryad.b8gtht7jv)

Code availability

The study did not generate custom codes but made use of standard packages with ArcGIS (v10.8), Origin (v2021) and SPSS Modeler (v18) software.

References

1. Laborde, D., Martin, W., Swinnen, J. & Vos, R. COVID-19 risks to global food security. *Science* **369**, 500–502 (2020).
2. Teeuwen, A. S., Meyer, M. A., Dou, Y. & Nelson, A. A systematic review of the impact of food security governance measures as simulated in modelling studies. *Nat. Food* **3**, 619–630 (2022).
3. Tilman, D. Global environmental impacts of agricultural expansion: the need for sustainable and efficient practices. *Proc. Natl. Acad. Sci. USA* **96**, 5995–6000 (1999).
4. Carvalho, F. P. Agriculture, pesticides, food security and food safety. *Environ. Sci. Policy* **9**, 685–692 (2006).
5. Ahrends, H. E. et al. Nutrient supply affects the yield stability of major European crops—a 50 year study. *Environ. Res. Lett.* **16**, 014003 (2021).
6. Chen, X. et al. Producing more grain with lower environmental costs. *Nature* **514**, 486–489 (2014).

7. Huang, Y. et al. Simulating no-tillage effects on crop yield and greenhouse gas emissions in Kentucky corn and soybean cropping systems: 1980–2018. *Agric. Syst.* **197**, 103355 (2022).

8. West, P. C. et al. Leverage points for improving global food security and the environment. *Science* **345**, 325–328 (2014).

9. Tilman, D., Balzer, C., Hill, J. & Befort, B. L. Global food demand and the sustainable intensification of agriculture. *Proc. Natl. Acad. Sci. USA* **108**, 20260–20264 (2011).

10. Foley, J. A. et al. Solutions for a cultivated planet. *Nature* **478**, 337–342 (2011).

11. Godfray, H. C. J. et al. Food security: the challenge of feeding 9 Billion people. *Science* **327**, 812–818 (2010).

12. Lambin, E. F. & Meyfroidt, P. Global land use change, economic globalization, and the looming land scarcity. *Proc. Natl. Acad. Sci. USA* **108**, 3465–3472 (2011).

13. Prosekov, A. Y. & Ivanova, S. A. Food security: the challenge of the present. *Geoforum* **91**, 73–77 (2018).

14. Jiao, X. et al. Grain production versus resource and environmental costs: towards increasing sustainability of nutrient use in China. *J. Exp. Bot.* **67**, 4935–4949 (2016).

15. Jiang, R. et al. Integrated soil nutrients management and China's food security. *Resour. Sci.* **30**, 415–422 (2008).

16. Zhu, Z. & Jin, J. Fertilizer use and food security in China. *J. Plant Nutr. Fertil.* **19**, 259–273 (2013).

17. Wang, J., Liu, Q., Ma, W., Rongfeng, J. & Zhang, F. Utilization and rational control measures of nutrient resources in China. *Resour. Sci.* **27**, 47–53 (2005).

18. Hou, M. et al. Estimation of fertilizer usage from main crops in China. *J. Agric. Resour. Environ.* **34**, 8 (2017).

19. Fu, H., Li, T., Cao, H. & Zhang, W. Research on the driving factors of fertilizer reduction in China. *J. Plant Nutr. Fertil.* **26**, 561–580 (2020).

20. Qiu, Z., Shen, W. S. & Lin, X. G. Chemical fertilizer reduction technology and its agronomic and ecological environment effects. *Soils Fertil. Sci. China*, **4**, 237–248 (2022).

21. Gebbers, R. & Adamchuk, V. I. Precision agriculture and food security. *Science* **327**, 828–831 (2010).

22. Yang, J. & Lin, Y. Spatiotemporal evolution and driving factors of fertilizer reduction control in Zhejiang Province. *Sci. Total Environ.* **660**, 650–659 (2019).

23. Shen, R., Wang, C. & Sun, B. Soil related scientific and technological problems in implementing strategy of "Storing Grain in Land and Technology". *Bull. Chin. Acad. Sci.* **33**, 135–144 (2018).

24. Chuan, L.-M., He, P. & Zhao, T.-K. Research advance on recommendation for crop fertilization methodology. *J Agric. Sci.Technol.* **18**, 95–102 (2016).

25. TONG, Q.-Q. et al. *Management Subarea of Paddy Soil Nutrients Based on GIS in Guizhou. Southwest China J. Agric. Sci.* 30,2727–2731 (2017).

26. Iizumi, T. et al. Prediction of seasonal climate-induced variations in global food production. *Nat. Clim. Change* **3**, 904–908 (2013).

27. Ghosh, K. et al. Development of crop yield forecast models under FASAL-a case study of kharif rice in West Bengal. *J. Agrometeorol.* **16**, 1 (2014).

28. Chen, S. et al. Weather records from recent years performed better than analogue years when merging with real-time weather measurements for dynamic within-season predictions of rainfed maize yield. *Agric. For. Meteorol.* **315**, 108810 (2022).

29. Zhang, L. et al. Using boosted tree regression and artificial neural networks to forecast upland rice yield under climate change in Sahel. *Comput. Electron. Agric.* **166**, 105031 (2019).

30. Timsina, J. & Humphreys, E. Performance of CERES-Rice and CERES-Wheat models in rice–wheat systems: a review. *Agric. Syst.* **90**, 5–31 (2006).

31. Kroes, J. et al. SWAP version 4. Report No. 1566-7197, (Wageningen Environmental Research, 2017).

32. Vanuytrecht, E. et al. AquaCrop: FAO's crop water productivity and yield response model. *Environ. Modell. Software* **62**, 351–360 (2014).

33. Martins, M. A. et al. Improving drought management in the Brazilian semiarid through crop forecasting. *Agric. Syst.* **160**, 21–30 (2018).

34. Mokhtari, A., Noory, H. & Vazifedoust, M. Improving crop yield estimation by assimilating LAI and inputting satellite-based surface incoming solar radiation into SWAP model. *Agric. For. Meteorol.* **250**, 159–170 (2018).

35. Wang, Y. & Gong, Y. Spectral remote sensing technology applied in crop yield estimation: research progress. *Chin. Agric. Sci. Bull.* **35**, 69–75 (2019).

36. Ferencz, C. et al. Crop yield estimation by satellite remote sensing. *Int. J. Remote Sens.* **25**, 4113–4149 (2004).

37. Singh, R., Semwal, D. P., Rai, A. & Chhikara, R. S. Small area estimation of crop yield using remote sensing satellite data. *Int. J. Remote Sens.* **23**, 49–56 (2002).

38. Chen, C., Zhu, X., Cai, Y. & Guo, H. A hybrid yield estimation model based on the trend yield model and remote sensing correction yield model. *Sci. Agric. Sin.* **50**, 1792–1801 (2017).

39. Zhou, Q. & Ismaeel, A. Integration of maximum crop response with machine learning regression model to timely estimate crop yield. *Geo-spatial Inform. Sci.* **24**, 474–483 (2021).

40. LI, P. et al. Assessment of terrestrial laser scanning and hyperspectral remote sensing for the estimation of rice grain yield. *Sci. Agric. Sin.* **54**, 2965–2976 (2021).

41. Zhang, J., Fang, S. & Liu, H. Machine learning approach for estimation of crop yield combining use of optical and microwave remote sensing data. *J. Geo-Inform. Sci.* **23**, 1082–1091 (2021).

42. Wang, Y. et al. An improved CASA model for estimating winter wheat yield from remote sensing images. *Remote Sens.* **11**, 1088 (2019).

43. Sun, Y.-Y. & Shen, S.-H. Research progress in application of crop growth models. *Chin. J. Agrometeorol.* **40**, 444–459 (2019).

44. Tao, S., Pan, J. & Liu, K. The application progress of DSSAT in field of agriculture and climate change in China. *Chin. Agric. Sci. Bull.* **31**, 200–206 (2015).

45. de Wit, A. et al. 25 years of the WOFOST cropping systems model. *Agric. Syst.* **168**, 154–167 (2019).

46. Zhao, Y. et al. Research Progress of APSIM model and its application in China. *Chin. Agric. Sci. Bull.* **33**, 1–6 (2017).

47. Bouman, M. & Laar, H. in *Los Baños: International Rice Research Institute, & Wageningen: Wageningen University & Research Centre, 235 Pp + Cd-rom.*

48. Zhu, Y. et al. Research progress on the crop growth model cropgrow. *Sci. Agric. Sin.* **53**, 3235–3256 (2020).

49. Van Klompenburg, T., Kassahun, A. & Catal, C. Crop yield prediction using machine learning: a systematic literature review. *Comput. Electron. Agric.* **177**, 105709 (2020).

50. Chipanshi, A. et al. Evaluation of the Integrated Canadian Crop Yield Forecaster (ICCYF) model for in-season prediction of crop yield across the Canadian agricultural landscape. *Agric. For. Meteorol.* **206**, 137–150 (2015).

51. Satir, O. & Berberoglu, S. Crop yield prediction under soil salinity using satellite derived vegetation indices. *Field Crops Res.* **192**, 134–143 (2016).

52. Filippi, P. et al. An approach to forecast grain crop yield using multi-layered, multi-farm data sets and machine learning. *Precis. Agric.* **20**, 1015–1029 (2019).

53. Paudel, D. et al. Machine learning for regional crop yield forecasting in Europe. *Field Crops Res.* **276**, 108377 (2022).

54. Li, L. et al. Crop yield forecasting and associated optimum lead time analysis based on multi-source environmental data across China. *Agric. For. Meteorol.* **308-309**, 108558 (2021).

55. Xu, H. et al. Machine learning approaches can reduce environmental data requirements for regional yield potential simulation. *Eur. J. Agron.* **129**, 126335 (2021).

56. Gómez, D., Salvador, P., Sanz, J. & Casanova, J. L. Modelling wheat yield with antecedent information, satellite and climate data using machine learning methods in Mexico. *Agric. For. Meteorol.* **300**, 108317 (2021).

57. Su, Y.-X., Xu, H. & Yan, L.-J. Support vector machine-based open crop model (SBOCM): Case of rice production in China. *Saudi J. Biol. Sci.* **24**, 537–547 (2017).

58. Nyéki, A. et al. Application of spatio-temporal data in site-specific maize yield prediction with machine learning methods. *Precis. Agric.* **22**, 1397–1415 (2021).

59. Cao, J. et al. Integrating multi-source data for rice yield prediction across china using machine learning and deep learning approaches. *Agric. For. Meteorol.* **297**, 108275 (2021).

60. van Grinsven, H. J. M. et al. Establishing long-term nitrogen response of global cereals to assess sustainable fertilizer rates. *Nat. Food* **3**, 122–132 (2022).

61. Correndo, A. A. et al. Assessing the uncertainty of maize yield without nitrogen fertilization. *Field Crops Res.* **260**, 107985 (2021).

62. Xu, X. et al. Spatial variation of attainable yield and fertilizer requirements for maize at the regional scale in China. *Field Crops Res.* **203**, 8–15 (2017).

63. Folberth, C. et al. Uncertainty in soil data can outweigh climate impact signals in global crop yield simulations. *Nat. Commun.* **7**, 11872 (2016).

64. Zhang, M., Li, J., Kong, Q. & Yan, F. Progress and prospect of the study on crop-response-to-fertilization function model. *Acta Pedolo. Sin.* **53**, 1343–1356 (2016).

65. Zhao, Y.-N. et al. GIS-based NPK recommendation and fertilizer formulae for wheat production in different regions of Henan Province. *J. Plant Nutr. Fertil.* **27**, 938–948 (2021).

66. Huang, Q., Dang, H., Huang, T., Hou, S. & Wang, Z. Evaluation of farmers' fertilizer application and fertilizer reduction potentials in major wheat production regions of China. *Sci. Agric. Sin.* **53**, 4816–4834 (2020).

67. Gong, L. et al. Analysis of chemical fertilizer application reduction potential for paddy rice in liaoning province. *Sci. Agric. Sin.* **54**, 1926–1936 (2021).

68. Yang, Y.-M., Huang, S.-H., Yang, J.-F. & JIA, L.-l. Analysis of wheat fertilizer reduction potential in Hebei province. *Soil Fertil. Sci. China.* **4**, 148–153 (2021).

69. Geng, W., Yuan, M., Wu, G., Wang, J. & Sun, Y. Study on the input and demand of crop nutrients and the potential of fertilizer reduction in Anhui Province. *Chin. J. Eco-Agric.* **28**, 221 (2020).

70. Zhang, G.-M. et al. Estimation of chemical fertilizer reduction potential for paddy rice using Gaussian-categorical mixture clustering methods. *J. Plant Nutr. Fertil.* **26**, 635–645 (2020).

71. Sun, B. et al. Research progress on impact mechanisms of cultivated land fertility on nutrient use of chemical fertilizers and their regulation. *Soils* **49**, 209–216 (2017).

72. Liang, T. et al. Response of rice yield to inherent soil productivity of paddies and fertilization in Sichuan Basin. *Sci. Agric. Sin.* **48**, 4759–4768 (2015).

73. Zhang, J.-P. & Qin, Y.-C. Spatial heterogeneity of grain yield per hectare and factors of production inputs in counties: a case study of henan province. *J. Nat. Resour.* **26**, 373–381 (2011).

74. Xu, X. et al. Spatial variation of yield response and fertilizer requirements on regional scale for irrigated rice in China. *Sci. Rep.* **9**, 3589 (2019).

75. Guo, Y. et al. Integrated phenology and climate in rice yields prediction using machine learning methods. *Ecolo. Indic.* **120**, 106935 (2021).

76. Sun, S., Zhang, L., Chen, Z. & Sun, J. Advances in AquaCrop model research and application. *Sci. Agric. Sin.* **50**, 3286–3299 (2017).

77. Wang, T., Yuan, S. & Wang, J. Study on vulnerability of drought hazard affected rice in Sichuan Province. *J. Nat. Disasters.* **22**, 221–226 (2013).

78. Deutsch, C. A. et al. Increase in crop losses to insect pests in a warming climate. *Science* **361**, 916–919 (2018).

79. Wang, B. et al. Sources of uncertainty for wheat yield projections under future climate are site-specific. *Nat. Food* **1**, 720–728 (2020).

80. Bullock, D. S. et al. The data-intensive farm management project: changing agronomic research through on-farm precision experimentation. *Agron. J.* **111**, 2736–2746 (2019).

81. Lacoste, M. et al. On-farm experimentation to transform global agriculture. *Nat. Food* **3**, 11–18 (2022).

82. Wang, Z. et al. Evaluating the effects of nitrogen deposition on rice ecosystems across China. *Agric. Ecosyst. Environ.* 285, https://doi.org/10.1016/j.agee.2019.106617 (2019).

83. YI, J. et al. The effects of chemical pesticide reduction on the occurrence of diseases, pests, weeds and rice yield. *Chin. J. Eco-Agric.* **28**, 11 (2020).

84. Cai, S. et al. Optimal nitrogen rate strategy for sustainable rice production in China. *Nature* **615**, 73–79 (2023).

85. Zhang, X. et al. Quantification of global and national nitrogen budgets for crop production. *Nat. Food* **2**, 529–540 (2021).

86. Wang, Q. et al. Spatial and temporal variation characteristics of the main agricultural inputs in sichuan province and the influencing factors. *J. Ecol. Rural Environ.* **34**, 717–725 (2018).

87. Tian, R. et al. Environmental risk assessment and trend simulation of non-point source pollution of chemical fertilization in Sichuan Province, China. *Chin. J. Eco-Agric.* **26**, 1739 (2018).

88. Li, J., Zhang, M., Xu, W., Kong, Q. & Yao, B. Principal component regression technology of ternary fertilizer response model for improving success rate of modeling. *Acta Pedol. Sin.* **55**, 467–478 (2018).

89. Goovaerts, P. Geostatistics in soil science: state-of-the-art and perspectives. *Geoderma* **89**, 1–45 (1999).

90. Liu, Q.-x et al. Analysis of spatial distribution and influencing factors of nitrogen and phosphorus fertilizer application intensity in Chengdu Plain. *Environ. Sci.* **42**, 3556–3565 (2021).

91. Xu, X. China GDP spatial distribution kilometer grid dataset. *Data Registration and Publishing System of the Resource and Environmental Science Data Center of the Chinese Academy of Sciences* (http://www.resdc.cn/DOI), https://doi.org/10.12078/2017121102 (2017).

92. Xu, X. China's population spatial distribution kilometer grid dataset. *Data Registration and Publishing System of the Resource and Environmental Science Data Center of the Chinese Academy of Sciences* (http://www.resdc.cn/DOI), https://doi.org/10.12078/2017121101 (2017).

93. Xu, X. China Annual Vegetation Index (NDVI) spatial distribution dataset. *Data Registration and Publishing System of the Resource and Environmental Science Data Center of the Chinese Academy of Sciences* (http://www.resdc.cn/DOI), https://doi.org/10.12078/2018060601 (2018).

94. Xu, X., Liu, L. & Cai, H. China's Farmland Production Potential Data Set. *Data Registration and Publishing System of the Resource and Environmental Science Data Center of the Chinese Academy of Sciences* (http://www.resdc.cn/DOI), https://doi.org/10.12078/2017122301 (2017).

95. Trevisan, R. G., Bullock, D. S. & Martin, N. F. Spatial variability of crop responses to agronomic inputs in on-farm precision experimentation. *Precis. Agric.* **22**, 342–363 (2021).

96. Yaddanapudi, R. & Mishra, A. K. Compound impact of drought and COVID-19 on agriculture yield in the USA. *Sci. Total Environ.* **807**, 150801 (2022).

97. Yang, S.-H., Zhang, H.-T., Guo, L. & Ren, Y. Spatial interpolation of soil organic matter using regression Kriging and geographically weighted regression Kriging. *Chin. J. Appl. Ecol.* **26**, 1649–1656 (2015).

98. Zou, Y.-B., Xia, B., Jiang, P., Xie, X.-B. & Huang, M. Discussion on the theory and methods for determining the target yield in rice production. *Sci. Agric. Sin.* **48**, 4021–4032 (2015).

99. Liao, Y.-l et al. Effects of long-term fertilization on basic soil productivity and nutrient use efficiency in paddy soils. *J Plant Nutr. Fertil.* **22**, 1249–1258 (2016).

100. Zhang, C., Tang, Y., Xu, X. & Kiely, G. Towards spatial geochemical modelling: use of geographically weighted regression for mapping soil organic carbon contents in Ireland. *Appl. Geochem.* **26**, 1239–1248 (2011).

101. Zhang, N., Zhang, Q., YU, H., Cheng, M. & Dong, S. Sensitivity analysis for parameters of crop growth simulation model. *J. Zhejiang Univ. (Agric. Life Sci.)* **44**, 107–115 (2018).

102. Yin, C.-M., Xie, X.-L. & Zhong, S.-L. Effect of different fertilizer applications on sustainable soil fertility and rice production in red soil paddy ecosystem. *Acta Ecolo. Sin.* **29**, 3059 (2009).

103. Sun, B.-H. et al. Evaluation on the sustainability of cropland under different long-term fertilization in Eum-Orthic Anthrosols area. *J. Plant Nutr. Fertil.* **21**, 1403–1412 (2015).

104. JI, J. et al. Changes in yield and fertilizer use efficiency of spring maize in Heilongjiang Province over a twenty year period. *J. Agric. Resour. Environ.* **39**, 1099–1105 (2022).

105. Deng, X., Deng, J., Wang, L., Gong, X. & Li, T. Effects of NPK fertilizers combined on agronomic traits,yield,nutrient uptake and utilization of "Heyu 9566" Maize. *Crops* **32**, 156–161 (2016).

106. Liu, X. & Li, S. Temporal and spatial distribution characteristics of crop straw nutrient resources and returning to farmland in China. *Trans. Chin. Soc. Agric. Eng.* **33**, 1–19 (2017).

107. Zhao, H., Zhao, X., Xie, L. & Guo, X. Spatial variation and its affecting factors of rice fertilizer use efficiency in Shangrao City of Jiangxi Province. *Acta Pedol. Sin.* **51**, 21–31 (2014).

108. Zhang, F. et al. Nutrient use efficiencies of major cereal crops in china and measures for improvement. *Acta Pedol. Sin.* **45**, 915–924 (2008).

109. Shao, H., Zhu, A., Shi, Q. & Zhao, X. Study on the recommended nitrogen fertilization system of rice in Jiangxi province. *Soil Fertil. Sci. China.* **5**, 55–60 (2016).

110. Cui, Z. Soil nutrient balance in rice−wheat rotation system in Taizhou City of Jiangsu Province. *J. Plant Nutr. Fertil.* **25**, 1002–1009 (2019).

111. Kohonen, T. *Self-organizing maps*. Vol. 30 (Springer Science & Business Media, 2012).

112. Jiang, Z., Chen, W. & Zheng, J. Study on temporal-spatial allocation zoning of land reclamation based on SOFM Neural Network. *China Land Sci.* **33**, 89–97 (2019).

113. Ma, C., Li, S., Liu, J., Gao, Y. & Wang, Y. Regionalization of ecosystem services of Beijing-Tianjin-Hebei Area based on SOFM neural network. *Prog. Geograp.* **32**, 1383–1393 (2013).

Author contributions
G.T.L. and T.X.L. conceived and led the project. G.T.L., T.X.L. and Y.D.W. designed the experiments and methodology. H.Y.Y. analyzed the field experiment data. P.H. and Z.Y.L. contributed data and produced the maps. T.F.D. contributed data and analyzed the soil data. C.H.X. revised the manuscript language. G.T.L. wrote and revised the manuscript. All authors discussed results and implications and commented on the manuscript at all stages.

Competing interests
The authors declare no competing interests

Additional information
Supplementary information The online version contains supplementary material available at https://doi.org/10.1038/s43247-023-01036-5.

Correspondence and requests for materials should be addressed to Guitang Liao or Tinxuan Li.

Peer review information *Communications Earth & Environment* thanks Brittani Edge and the other, anonymous, reviewer(s) for their contribution to the peer review of this work. Primary Handling Editors: Fiona Tang, Martina Grecequet and Aliénor Lavergne. A peer review file is available.

Reprints and permission information is available at http://www.nature.com/reprints

Publisher's note Springer Nature remains neutral with regard to jurisdictional claims in published maps and institutional affiliations.